Structural and sedimentary origin of the Gargano - Pelagosa gateway and impact on sedimentary evolution during the Messinian Salinity Crisis

Structural and Sedimentary Origin of the Gargano - Pelagosa Gateway and Impact on Sedimentary Evolution during the Messinian Salinity Crisis

Romain Pellen[1], Daniel Aslanian[2], Marina Rabineau[1], Jean-Pierre Suc[3], William Cavazza[4], Speranta-Maria Popescu[5], Jean-Loup Rubino[3].

[1] Laboratoire Geo-Océan, Institut Universitaire Européen de la Mer, UMR6538, Rue Dumont d'Urville, 29280 Plouzané, France.
[2] IFREMER, Laboratoire Geo-Ocean - Géodynamique et Enregistrement Sédimentaire, 1 place Nicolas Copernic, 29280 Plouzané, France
[3] Institut des Sciences de la Terre Paris (ISTEP), UMR 7193, Laboratoire Evolution et Modélisation des Bassins Sédimentaires, Université P. et M. Curie - Paris 6, 75005 Paris, France
[4] Department of Biological, Geological, and Environmental Sciences; Piazza di Porta S.Donato 1, 40100 Bologna, Italia
[5] GeoBioStrataData consulting ; 385 Route du Mas Rillier, 69140 Rillieux la Pape, France.

Abstract

Circulation of water masses, sediment, and biotope between the sub-basins of the Mediterranean Sea strongly depends on morphological oceanic gateways. These geological features react to geodynamic reorganisation through volcanism, vertical movements, and/or the segmentation of sedimentary basins. Despite the palaeogeographic relevance of straits and oceanic-gateways, their evolution and impact on sedimentary transports and deposition in the Mediterranean remain in general poorly constrained. The Gargano-Pelagosa gateway is here first recognized as an influential element of the palaeogeographic/environmental evolution of the central-southern Apenninic foredeep and wedge-top domains during the Messinian, as shown by the integration of (i) seismic lines, (ii) well information from the Adriatic Sea, and (iii) a review of both onshore and offshore structural data and Messinian depositional environments. A palinspastic evolution is proposed for the Apennine and south Adriatic foredeeps during the Messinian Salinity Crisis (MSC: 5.97-5.33 Ma). We highlight the implication of the pre-MSC structural legacy and the development of the Apennine and Dinarid-Albanian chains in 1) the isolation of the Apennine foredeep from the deep central Mediterranean domains at the peak of the MSC; 2) the vertical movements at the Gargano-Pelagosa structure and the Apulian Platform and 3) their implication in the deposition of a chaotic sedimentary body.

Keywords: Mediterranean Sea, Segmented basin, Marine pathways, Messinian Salinity Crisis, Palaeogeographic and Palinspastic reconstruction.

Introduction

The paleocurrents, and therefore the evolution of the paleoclimate but also of the dispersal of sediments and their deposition, is strongly linked to the presence and evolution of straits which can act as open passages (oceanic gateways) or barriers (Straume *et al.*, 2020). In the Mediterranean Sea, the present-day physiographic map shows a strong segmentation with several major oceanic gateways (i.e. the Gibraltar, Sicilian, Aegean straits) and secondary oceanic gateways (Figure 1). As circulation of water masses, sediment, and biotope between the sub-basins of the Mediterranean Sea strongly depends on these morphological oceanic-gateways, their evolution is of primary importance to understand the morphological and sedimentary evolution of the different basins (e.g. Leever *et al.*, 2010; Flecker *et al.*, 2015; Palcu *et al.*, 2017; Suc *et al.*, 2015; Balázs *et al.*, 2017, Pellen et a., 2017; Amadori *et al.*, 2018; Camerlenghi *et al.*, 2020). This is particulary critical in the case of large relative sea-level variations, such as during the MSC (5.97–5.33Ma) (Manzi *et al.*, 2013) when huge amount of gypsum was only deposited along the Apennine Foreland (Manzi *et al.*, 2020), and a understanding approach of the Mediterranean Sea needs very detailled local studies, such as for the Betic, Rifain, Balkan or Iron Gate gateways (Figure 1; Betzler *et al.*, 2006; Krijgsman *et al.*, 2006; Suc *et al.*, 2011, 2015; Do Couto *et al.*, 2016).

The Gargano-Pelagosa gateway, located on the Adria plate and separating the central and the south Adriatic basins, perfectly displays the relationship between the inherited sedimentary structure (e.g. Argnani, 2013), vertical tectonic motion and sea-level variation, and their impacts on water mass exchange during the Neogene. To understand the relationship between each process, we focus on the connection between the Adriatic foredeep, the South Adriatic Basin (SAB) and the deep Ionian Sea (through the former Lagonegro Basin) during the Messinian Salinity Crisis (MSC: 5.97-5.33 Ma) taking account of the pre-MSC inherited sedimentary and/or tectonic features.

In this study, we describe the segmentation and tectonic history of each domain surrounding the Gargano-Pelagosa gateway by compiling the onshore and offshore structural and sedimentary features. These observations are completed by the compilation of borehole data and seismic profiles between the Central Adriatic Basin (CAB) and the South Adriatic Basin (SAB).

This set of data allowed us to re-evaluate the relationships of MSC environment history with the structural heritage and to present palinspastic and environmental reconstructions for the Messinian period.

Regional setting

1. Early history of the Adria plate

The present-day structure of the central Mediterranean area and the Adria plate results from the interaction between the African, European, Iberic and Adria plates since the breakup of the mega-continent Pangea (for a review, see Cavazza *et al.*, 2004).

Mesozoic palaeogeographic reconstructions suggest two main sub-orthogonal extensional directions associated with the development of Neotethysian oceanic domains: NW-SE and NE-SW (Ciarapica and Passeri, 2002; in Vezzani et al, 2010; Stampfli and Hochard, 2009). Associated to these orientations several present-day NW-SE oriented carbonate platform and basin systems have been identified (Figure 2; Zappaterra, 1994; Wrigley *et al.*, 2015; Vezzani *et al.*, 2010). The present-day situation and stratigraphic evolution of each platform and basin-slope/deep-basin systems developed during Mesozoic and Cenozoic time is presented in figures 2 and 3. Even if the nature, age and orientation of the Ionian Sea remain a subject of debate (see Dercourt, 1972; Channell *et al.*, 1980; Mele, 2001; Panza *et al.*, 2003; Vezzani *et al.*, 2010; Roure *et al.*, 2012; Carminati *et al.*, 2012; Dellong *et al.*, 2018; van Hinsbergen *et al.*, 2020), northward extension have been associated to this domain such as the south Adriatic Sea or the deformed Mesozoic Sannio-Molise and Lagonegro basins.

2. A multi-segmented peri-Adriatic domain

The eastern border of the Adria plate is associated to the Dinarid and Albanid-Hellenid fold-and-thrust belts (Figure 2). The Scutari-Pec lineament separates the two fold-and-thrust belts and is interpreted as a major dextral polyphasic transform fault system (Figure 2; Chorowicz *et al.*, 1981; Grubic and Marovic, 1991) developed during Cretaceous and Cenozoic time. The Dinarid chains was mainly formed during Eocene – Oligocene time and incorporates large parts of the Adriatic-Dinaric platform systems (e.g. Schmid *et al.*, 2008; Stampfli and Hochard, 2009; Korbar, 2009; Handy *et al.*, 2010; van Hinsbergen *et al.*, 2020). The Albanid-Hellenid chain underwent two supplementary tectonic and exhumation stages - from the Middle-Late Miocene until the present-day (Kilias *et al.*, 2001; Frasheri *et al.*, 2009; Pashko and Aliaj, 2020). During the Neogene,

two subsidence phases are recorded leading to the formation of the South Adriatic foredeep domain, the first in the Middle Miocene-Tortonian (Pannonian-Tortonian stage), and the second in the Late Miocene-Pliocene (Pontian s.l.). The two phases are separated by a short compressive phase at the Late Miocene (Pashko and Aliaj, 2020). At the scale of the Albanid-Hellenide chain, the system would be affected by several phases of counterclockwise rotations, and estimated at 40°ccw between 15-13 and 8 Ma and 10°ccw in the Late Miocene-Pliocene (van Hinsbergen *et al.*, 2005; Frasheri *et al.*, 2009).

On the western border the Apennine system is part of a wide peri-Mediterranean orogenic system developed from late Oligocene to present, associated with the counter-clockwise rotation of the Corsica-Sardinia blocks during the Early Miocene, and Tyrrhenian Basin opening since Middle-Late Miocene (e.g. Ricci Lucchi, 1986; Boccaletti *et al.*, 1990). Figure 3 summarize the deformation stage associated to each Mesozoic palaeogeographic domain now involved in the Central and South Apennine Chain, Several tectonic phases are reported, each one implying the folding and imbrication of the cover succession detached toward the foreland, and the progressive involvement of younger and easternmost fore-deep basins (Casero, 2004; Ghielmi *et al.*, 2010; Vezzani *et al.*, 2010; Artoni, 2013) (Figures 2 and 3).

The Central Apennines are delimited to the south by the Anzio-Ancona (A.A.) and Maiella-Roccamonfina (M.R.) lineaments (Figure 2). The Central Apennine chain accreted the Mesozoic Tuscany and Umbria-Marche pelagic domains (Figures 2 and 3 - Vezzani *et al.*, 2010; Fantoni and Franciosi, 2010). Several Neogene tectonic phases are recorded along the Apennine and are associated to the development of several foreland basins (see Figure 3 and Ghielmi *et al.*, 2010; Vezzani *et al.*, 2010 for further information), which were gradually cannibalized by the Apennine chain.

The Southern Apennine Chain is delimited by the Anzio-Ancona lineament (A.A.) to the north and the Calabria block to the south (Figures 2). The Neogene stratigraphy has been widely studied (see Vezzani *et al.*, 2010; Ascione *et al.*, 2012; Vitale and Ciarcia, 2013 for further detail) and related palaeoenvironmental domains have been associated with the inherited Mesozoic domains (Vezzani *et al.*, 2010; Figure 3). The first signs of Neogene deformation along the Apennine platforms are dated to post-Burdigalian-Langhian (Figure 3). From late Tortonian-early Messinian, the whole tectonic wedge, including the Apennine Platform, overthrust the Sannio-Molise and Lagonegro basins (Cippitelli, 2007; Vitale and Ciarcia, 2013). This new tectonic phase

implies the development of fore-deep successions along the Lagonegro basin, until the late Messinian (Figure 3).

Since late Messinian several thrust fronts are activated along the south and central Apennine fold-and-thrust belt led to the progressive incorporation of the Messinian foredeep (including the Messinian Laga Basin) into the belt and marked the initiation of a late Messinian-early Pliocene foredeeps (Figure 3; Milli *et al.*, 2007; Vezzani *et al.*, 2010; Artoni, 2013).

3. Structural features affecting the Gargano-Pelagosa gateway

Several structural features affect the Gargano Peninsula and Palagruža Island (Figure 2), which mark the boundary between the south (SAB) and central (CAB) Adriatic basins. The Gargano Peninsula is part of the Apulian foreland, the most uplifted portion of a wide NW-SE trending flexural antiform influenced by both the SW-verging Dinaric-Hellenic and NE-verging Southern Apennine orogens (Moretti and Royden, 1987; Argnani *et al.*, 1993; Hairabian *et al.*, 2015). Around the Gargano Peninsula at least three main structural features have been described, but their relationship remains debated:

- **The Mid Adriatic Ridge (MAR),** developed along a general NW-SE axis, at the interface of the Apennine and Dinarid deformation fronts (Figure 2) (Finetti, 1982; Argnani and Gamberi, 1995). It consists of an array of structural highs, 10-40 km wavelength anticlinal structures and Triassic salt diapirism structures (Casero and Bigi, 2012). Sub-basins comprised between salt structures observe Triassic to Miocene sedimentary layers and highlight the salt diapir growth phase through time (Festa *et al.*, 2013).
- The SW-NE oriented **Tremiti Ridge** located north of the Apulian Platform and is defined by Triassic salt diapirism (Figure 2). A Late Miocene deformation period have been identified along this structural feature (e.g. Festa *et al.*, 2013), but not excluding earlier phases during Cenozoic and Mesozoic. Sedimentary hiatus on top of the Tremiti ridge suggest repeated emersion during Paleocene, Oligocene, and Messinian times (Andriani *et al.*, 2005).
- **The Mattinata Fault System** (MFS) is observed both on land and at sea (e.g. Argnani *et al.*, 2009; Billi *et al.*, 2007; Figure 2). The offshore Mesozoic and Tertiary succession defines a series of E-W to NE-SW trending anticlines. Secondary anticlinal axes, oriented NW-SE, are located south of the Mattinata system and connect further north to the main system. The system extends onshore within the Gargano Peninsula promontory and delimits two former Mesozoic shallow and deep environment domains by a NW-SE axis faulted system: the western part is

141 associated to Mesozoic carbonate platform deposit of the Apulian Platform and the eastern part
142 to slope-deep Mesozoic carbonate deposit. Several tectonic reactivations and strike-slip motions
143 linked to regional and tectonic phases are documented (Morelli, 2002; Argnani *et al.*, 2009).
144
145 The relationship between the MAR, the Tremiti Ridge and the MFS remains uncertain, as
146 well as the importance of these features in a wider geodynamic framework or the possible
147 involvement of the Hercynian basement (Fantoni and Franciosi, 2008, 2010). These structures
148 have been interpreted as a micro-plate boundary linked to reorganisation of forces at the limits
149 of the Adria microplates (Scisciani and Calamita, 2009), or as an eastward verging fault system
150 delimiting the external Apennine deformation front (Bally *et al.*, 1986; Ori *et al.*, 1991; De
151 Alteriis, 1995; Scrocca, 2006; Casero and Bigi, 2012) and connected to the Apennine front
152 through the Tremiti Ridge (Funiciello *et al.*, 1991; Festa *et al.*, 2013). Crustal thickness modeling's
153 suggest a thinner continental crust (~30 km) at the CAB-SAB transition (Ritzwoller *et al.*, 2007),
154 as well as a shallower Moho depth from the CAB to the SAB (Moho rise from 30 to 20 km;
155 Riguzzi and Doglioni, 2020). No sharp discontinuities are highlighted by tomographic modelling,
156 but this does not invalidate the possibility of deep crustal structures or geodynamic hinge line as
157 observed by geophysical data in the Liguria-Provence or Valencia basins (e.g. Afilhado *et al.*, 2015;
158 Moulin *et al.*, 2015; Leroux *et al.*, 2015a, b; Pellen *et al.*, 2016).

159 The extension of the MAR towards the SAB is also problematic due to its possible
160 interaction with the Tremiti Ridge, and its proximity to the Gargano peninsula and the Mattinata
161 Fault System. In any case, these structures influence the vertical evolution of the Gargano
162 promontory and the marine corridor between CAB and SAB during tectonic reorganisation
163 phases (Festa *et al.*, 2013). These movements have been suggested during the Cenozoic and Late
164 Miocene (Scisciani and Calamita, 2009; Argnani *et al.*, 2009; Festa *et al.*, 2013), but have not
165 been quantified. Argnani *et al.* (2009) suggested that the development of the MSC succession
166 west of the Mattinata fault system and the MAR could be assigned to a change of motion along
167 the MFS from sinistral to dextral strike-slip motion. While the orientation and character of the
168 different Mesozoic platform-basin domains primarily control the CAB-SAB connections, the
169 marine corridor is strongly influenced by these structures. However many questions remain as to
170 the origin of each structural features and role in the isolation of the CAB.

Understanding the oceanic gateways evolution helps us to understand why different sedimentary environments are observed on either side of the Gargano promontory during the different stages of the Messinian crisis, such as the presence and absence of halite deposition in the Caltanissetta and Po Plain basins respectively, although both basins presented similar water depths (Amadori *et al.*, 2018; Camerlenghi *et al.*, 2020).

4. Present-day observation of the Messinian deposits across the Adria plate

1. MSC evolution along the Adria plate

A consensus has been reached in the scientific community in subdividing the MSC into three main stages at the Mediterranean scale (between 5.97 and 5.33 Ma), each of them well time-constrained and characterized by specific evaporite deposits and palaeo-hydrological conditions (Clauzon *et al.*, 1997; CIESM, 2008; Roveri *et al.*, 2014; Manzi *et al.*, 2013, 2020). Nevertheless, in detail, this consensus is not so large considering the various options discussed in CIESM (2008) but restricted to one option only in Roveri *et al.* (2014). This is also demonstrated by recent investigations on deep Messinian basins using industry drilling results and seismo-stratigraphy (e.g. CIESM, 2008; Gorini *et al.*, 2015; Roveri *et al.*, 2016; Madof *et al.*, 2019; Andreetto *et al.*, 2021a,b), these three stages may not be applicable everywhere in deep water basins (essentially the Eastern Mediterranean and Levant basins). Accordingly, we follow the Bache *et al.* (2015)'s chronology which takes into account all the recent robust data:

- Stage 1 (5.97-5.60 Ma) is associated with the development of shallow-water primary evaporites (present only in marginal basins) (Clauzon *et al.*, 1997; CIESM, 2008), while organic-rich shales sedimented in deeper water (Manzi *et al.*, 2007). Up to 16 shale-gypsum cycles were deposited in relation to strong astronomical control and restriction of marine water connection between the Atlantic and Mediterranean domain through the Rifian and Betic corridors (Krijgsman *et al.*, 1996; Hilgen *et al.*, 2007; Lugli *et al.*, 2010).
- Stage 2 (5.60-5.55 Ma) marks the MSC paroxysm defined by the drastic marine water exchange restriction between the Atlantic and Mediterranean seas leading to an important sea-level drop in a hypersaline deep-basin system, sedimentary transfer to the deeper marine areas, and uplift and deep fluvial erosion along the marginal domains (Clauzon *et al.*, 1997). Estimates of sea-level drop magnitude at the Mediterranean scale range from 100-200 m (Manzi *et al.*, 2018) to 650-900 m (Amadori *et al.*, 2018; Ben-Moshe *et al.*, 2020), 1000 m

(Pellen *et al.*, 2019) or 1500 m (Clauzon *et al.*, 1997; Bache *et al.*, 2009; Lofi *et al.*, 2011), according to basin physiography and/or scenario hypotheses. The exact timing of deposition between east and west Mediterranean sub-basins and the presence of shallow vs. deep environments are still a matter of debate (Roveri *et al.*, 2014; Bache *et al.*, 2015; Gorini *et al.*, 2015).

– Stage 3: the timing of the Mediterranean marine reflooding (comprised between 5.55 and 5.33 Ma) also remains intensely debated (Andreetto *et al.*, 2021a; Popescu *et al.*, 2021) with a first numerical model proposing an ultra-rapid rise in sea level at the end of the Messinian event (Garcia-Castellanos *et al.*, 2009, 2020) and models proposing a stepwise reflooding of the Mediterranean domains based on seismic reflection data (Bache *et al.*, 2012, 2015; Gorini *et al.*, 2015). In this hypothesis, a late lowstand period (5.55 – 5.46 Ma) is proposed to explain the rapid precipitation of halite in the deep settings (Bache *et al.*, 2015; Gorini *et al.*, 2015). This phase is associated with a relatively slow sea level rise, which smoothed out the scarring of the MSC crisis producing a very flat marine ravinement surface. At 5.46 Ma, the rapid sea level rise helped to preserve the scars of the MSC crisis on the margin, later followed by a moderate sea-level rise at 5.33 Ma (Bache *et al.*, 2012; Popescu *et al.*, 2021). However, Bache *et al.* (2012) and Pellen *et al.* (2017) showed that the Mediterranean marine waters re-entered later the Apennine foredeep, at 5.36 Ma.

Figure 4 presents the present-day distribution of MSC-related deposits along the Adria plate compiled from the literature. The identification and description of Messinian formations have led to the subdivision of the Adria domain into three main subdomains: (1) the Central Adriatic Basin (CAB) fringed by the north and central Apennine chains, limited to the south by the Gargano Peninsula and Palagruža Island, (2) the south Apennine Chain bounded to the east by the Apulian Platform, and (3) the South Adriatic Basin (SAB) bounded to the south by the Otranto Strait and to the east by the outer Albanid front.

ii. The central Apennine foredeep and the Central Adriatic Basin

The Messinian stratigraphy of the CAB has been extensively studied with onshore and offshore sedimentary observations (Selli, 1960; Roveri *et al.*, 1998, 2001, 2004, 2008a,b; Milli *et al.*, 2006, 2007; Popescu *et al.*, 2007, 2008; Lugli *et al.*, 2010), geophysical observations (Ghielmi *et al.*, 2010, 2013; Rossi *et al.*, 2015), and land-sea correlations (e.g. Ori *et al.*, 1991; Artoni and Casero, 1997; Roveri and Manzi, 2006; Roveri *et al.*, 2005, 2008; Artoni, 2013; Pellen *et al.*,

2017; Manzi *et al.*, 2020). Significant effort has been made to simplify the Messinian lithostratigraphy at a regional scale (Roveri *et al.*, 2008, 2014) and to correlate onshore with offshore deposits. Table 1 summarizes the different studies and correlations of Messinian formations across the Central Apennine belt (Figure 4; Table 1). To simplify the description of the Messinian lithostratigraphy of each area across the Adria plate in this study, we adopted the nomenclature of Roveri *et al.* (2004, 2005).

The Messinian Apennine foredeep was formed by the migration of the Marnoso-arenacea foredeep during the Late Tortonian-Early Messinian tectonic phase, and includes three main depocenters along the CAB (Figure 4). Two megasequences (Table 1 ; T_2, MP, *sensu* Roveri *et al.*, 2005) have been associated with the Messinian Salinity Crisis and respectively dated between ca. 8Ma - 5.6 Ma, and 5.6 - 5.33 Ma.

The upper section of the T_2megasequence corresponds to the development in an active tectonic setting of 1) the primary evaporites (Primary Lower Gypsum – PLG) from 5.97 Ma to 5.6 Ma (stage 1) in marginal wedge-top basins and foreland domain (Vena del Gesso Fm., Roveri *et al.*, 2003, 2005, 2006; Rossi *et al.*, 2015; Manzi *et al.*, 2020 - Gessoso Solfifera Fm. (evaporate)) and 2) siliciclastic fan deltas which evolved laterally to anoxic clays and dolomicrites in the main depocenters (Milli *et al.*, 2006, 2007; Ghielmi *et al.*, 2010, 2013).

Associated with the MSC stage 2 and the reflooding step closing the crisis, the initiation of the MP megasequence (Table 1) corresponds to a wide stratigraphic unconformity dated at 5.60 Ma observed along the whole Apennine fold-and-thrust belt. This regional event is part of a major change of depocenters and is called "intra-Messinian phase" (Ciaranfi *et al.*, 1973; Elter *et al.*, 1975; Di Nocera *et al.*, 2006; Colalongo *et al.*, 1976; Roveri *et al.*, 2005; Milli *et al.*, 2007; Bigi *et al.*, 2009, 2011; Ghielmi *et al.*, 2010; Artoni, 2013). The eroded products of marginal domains were resedimented in deep basins (Resedimented Lower Gypsum – RLG, e.g. Roveri *et al.*, 2001; Artoni and Casero, 1997; Artoni, 2003, 2013; Roveri *et al.*, 2014; Milli *et al.*, 2007). These formations generate the general structure of $p-ev_1$ Fm (post-evaporate Fm.), which includes a regional scale rhyolitic cinerite dated at 5.532 +/-0.004Ma (Cosentino *et al.*, 2013). The $p-ev_1$ Fm. is devoid of fossils and mainly comprises thin-bedded siliciclastic turbidites considered to have been deposited in deep, freshwater conditions (Roveri *et al.*, 2001).

The base of the $p-ev_2$ Fm. is age debated (5.36 Ma in Popescu *et al.*, 2007; Bache *et al.*, 2012; Pellen *et al.*, 2017; 5.42 Ma *in* Roveri *et al.*, 2014; Manzi *et al.*, 2020) and could mark a change

from a regressive to transgressive trend in the post-evaporitic succession (Manzi *et al.*, 2020). The $p-ev_2$ Fm. is considered to have mostly been deposited in hypohaline conditions (Popescu *et al.*, 2007; Pellen *et al.*, 2017) and known for its content in Paratethyan fossils (Lago Mare biofacies; Selli, 1973; Colalongo *et al.*, 1976; Corradini and Biffi, 1988). Based on the study of microfossils, at least four marine incursions are associated with $p-ev_2$ Fm. (Popescu *et al.*, 2007 ; Pellen *et al.*, 2017), which probably later invaded the Po Basin (Channell *et al.*, 1994 ; Sprovieri *et al.*, 2008 ; Violanti *et al.*, 2007, 2011) due to the compartmentalization of the Apennine foredeep (Amadori *et al.*, 2018).

3. The east Apulian Platform and the south Apennine fold-and-thrust belt

Contrary to the Central Apennine Messinian foredeep, the MSC deposits identified along the South Apennine chain are located in a wedge-top depositional zone (Amore *et al.*, 1988; Chiocchini *et al.*, 2003; Pescatore *et al.*, 2008; Matano *et al.*, 2005, 2014; Barone *et al.*, 2006, 2008; Vezzani *et al.*, 2010; Ascione *et al.*, 2012) or along the Apulian foreland system (Pellen, 2016; Petrullo *et al.*, 2017; Manzi *et al.*, 2020).

On the foreland domain close to the Apulian Platform, the pre-MSC late Miocene succession presents several stratigraphic gaps during Paleocene, Oligocene, upper Langhian and Tortonian times (Vezzani *et al.*, 2010; Petrullo *et al.*, 2017). On the Apulian Platform, a syn- or post-Messinian breccia deposit directly overlies the upper Cretaceous to Middle Miocene carbonate formation (Figure 3; Pellen, 2016; Manzi *et al.*, 2020). Towards the western side of the Apulian foreland and below the allochthonous nappes, pre-evaporitic Messinian marls, primary evaporites and post-evaporite successions are preserved (Petrullo *et al.*, 2017).

The allochtonous domain of the South Apennine Chain observe preserved pre-MSC and MSC formations on top of the former Sannio-Lagonegro Mesozoic basin (Matano *et al.*, 2007; Vezzani *et al.*, 2010). Development of the MSC successions seems to occur in a syn-tectonic setting (Matano *et al.*, 2007, 2014) with 1) organic-rich marls and diatomites and 2) PLG (stage 1 of the MSC), partially eroded and overlapped either by RLG or Pliocene conglomerate deposits depending on the tectono-stratigraphic context of the outcrop (Matano *et al.*, 2007). The absence of MSC formation belonging to a deep environment and/or foredeep system below the present-day south Apennine Chain (Matano *et al.*, 2005, 2014; Matano, 2007; Manzi *et al.*, 2020) may suggest: 1) a shallow depositional environment along the Apulian Platform system with a cannibalized deep Lagonegro domain or 2) in the case of the presence of such deposits below the

296 south Apennine Chain, the possibility of a deeper Messinian depositional setting towards the
297 south of the Apulian Platform edge and Lagonegro domain.

298 The SAB is the least studied of the three areas. The SAB Messinian deposits seem
299 disconnected from those of the CAB and borehole information (Sparviero 001 borehole; Manzi
300 *et al.*, 2020) shows the initiation of resedimented gypsum formation located along the SAB. The
301 southward extension to the Ionian Sea through the Otronto Strait is still a matter of question
302 (Figure 4). According to the nomenclature of Lofi *et al.* (2018), these deposits are interpreted as
303 a detrital formation (Complex Unit - Manzi *et al.*, 2020; Upper Unit in Lofi *et al.*, 2011 of
304 unknown origin. Their mapping and the tectonic/sedimentary processes associated with
305 Messinian deposition in the SAB remain relatively unknown.

306 ## Data and methodology

307 To characterize the development of Cenozoic and MSC units along the Central Adriatic
308 Basin (CAB) and South Adriatic Basin (SAB), we merged seismic reflection profiles studied
309 during the academia-industry program GRI *Méditerranée* (Groupement Recherche-Industrie) and
310 vintage industrial profiles obtained from the VIDEPI website
311 (https://www.videpi.com/videpi/videpi.asp) and reprocessed. Figure 05 present the distribution
312 of the seismic lines used in this study and highlight the line drawings presented figures 7 and 8
313 (Non-interpreted seismic lines are illustrated in supplementary material 1 and 2). B The regional
314 distribution of these profiles allows us to re-evaluate the Neogene seismo-stratigraphy (Some of
315 the main Neogene seismic horizons based on Videpi seismic lines are published in Pellen *et al.*,
316 2021) and compare the development of the different stratigraphic unit identified along the CAB
317 and SAB. Information on available boreholes obtained from the VIDEPI website was also
318 integrated in order to calibrate and correlate the identified megasequences between the SAB and
319 CAB. This set of data led us to re-evaluate the relationships of MSC palaeo-environments history
320 with the structural and sedimentary heritage and to present a set of palinspastic and
321 palaeoenvironmental reconstruction maps for that period. These palinspastic maps were built
322 using Placa (Matias *et al.*, 2005) and Placa4D (Pelleau *et al.*, 2015) free softwares
323 (https://wwz.ifremer.fr/gm_eng/Products-and-services/Free-softwares).

324 Boreholes and seismic lines are illustrated in Figure 5, which combines the MSC
325 sedimentary formations described earlier along the CAB and South Apennine Chain, and the
326 new cartography of the MSC units detailed in this section. Table 2 presents the stratigraphic

charts used in this study for (i) borehole correlation along the Adriatic Sea (Figures 2, 6a and 6b) and (ii) seismic stratigraphic interpretation across the CAB (Figure 7) and SAB (Figure 8). Beyond the age of the stratigraphic units, their delimitations are based on the recognition of angular unconformities and erosive discontinuities.

Results

1. Post-Mesozoic sedimentary evolution between the CAB and SAB from borehole observation

i. Observed structural features

The Gargano Peninsula and Palagruža Island (see location in Figure 2) mark the boundary between the south (SAB) and central (CAB) Adriatic basins. The depth of the top of the Mesozoic series reached in boreholes varies markedly between 2400-2900m in the SAB and 1700-2000m in the CAB (Figures 6a, and 6b). The transition between the two basins is influenced by several structural features of different wavelengths.

The Gargano Peninsula is the most elevated portion of the Apulian foreland and is influenced 1) by a north-westward bending within the entire CAB (Figure 7 – SONE03-06) under the influence of the NE-verging Apennine orogeny and 2) to a south-eastward bending within the SAB under the influence of the SW-verging Dinaric-Hellenic orogeny (Figure 8 – SONE 09) (Moretti and Royden, 1987; Argnani *et al.*, 1993; Hairabian *et al.*, 2015).

Offshore observations confirm an antiformal structural high delimited by the MFS and the MAR (Figure 7-SONE07; Figure 8 – SONE08-09) which mainly affected Mesozoic formations. Towards the southeast, at the termination of the MFS and MAR, this structural high disappears (Figure 8 – SONE09). Deformation decreases on either side of these structures with the general development of Miocene depocenter (Figure 5; Figure 8 – NOSE02-04, SONE09). Towards the north and respectively west and east the MFS and MAR features surround the Gargano Peninsula (Figures 2, 5). The transition between the CAB and SAB corresponds to a narrow Mesozoic slope-to-basin corridor –cropping out on the eastern part of the Gargano Peninsula– and strongly deformed by the MAR Mesozoic to present-day deformation that can be observed along several seismic lines (Figure7 - SONE03-07; Figure 8 – NOSE05) and could be associated with the structural basement/Mesozoic dome and Triassic salt diapirism.

A minimum of 2 s twt difference in depth is observed between the undeformed basin domain and the structural crest (Figure 8 – SONE08 (km120)), suggesting >3 km uplift since the Late Cretaceous and affecting the Gargano Peninsula. These deformation pulses may correlate with the development of several sedimentary hiatuses (see next section). Together with the development of the MAR, one of the main impacts could be the disconnection between the CAB and SAB through the Gargano-Pelagosa corridor including during the MSC.

2. Post-Mesozoic to Miocene megasequences

Seven megasequences were defined from borehole correlation and seismic interpretation (Figures 6a, 6b, 7, 8, 9). In this study we have focused our description on three megasequences: the Paleocene-Eocene and Oligocene, Miocene pre-MSC, and Messinian syn-MSC megasequences.

The **Paleogene-Eocene and Oligocene** megasequences mainly developed at the foot of the slopes of ancient Mesozoic carbonate platforms (i.e. Fantoni and Franciosi, 2010) or along the Dinarid fold-and-thrust belt in preserved foredeep depocenters (Figures 7, 8 – NOSE03, SONE03-04-08). On the Apulian Platform, a sedimentary hiatus is observed at the top (Figure 6b, boreholes Sonia 001, Rovesti 001) and is locally associated with breccia deposits (Figure 6b, borehole Edgar 002). Sediment are mainly composed limestone and argillaceous limestone along the CAB. Important Paleogene-to-Oligocene depositional and/or erosional hiatuses are locally observed on the Apulian Platform (Figure 6b – Sonia 001) or east of the Gargano Peninsula on the uplifted part of the Mesozoic Ionian domain (Figure 6a – Cigno Mare). Casero and Bigi (2012) also observed a Late Mesozoic-Burdigalian depositional hiatus north of the Gargano Peninsula. Other boreholes from this area show older hiatuses from the Coniacian to the Tortonian (Gargano Mare 001; Pellen, 2016). Within the SAB, a hiatus is observed at the Late Cretaceous—Eocene interval (Figures 6a, 6b - Sparviero bis), followed by an important deposition of carbonate and silt-marl during the Miocene.

The **Aquitanian to Messinian pre-MSC megasequence of the CAB and SAB** is mainly developed along the SAB along the former basinal Mesozoic domain. It is divided into two sub-sequences: Aquitanian-Langhian (Bisciaro formation) and Serravallian-Tortonian (Schlier formation). It is one of the series marking the greatest difference between the CAB and the SAB. The Miocene sequence in the CAB is marked by a condensed set of clay carbonates (average thickness of about 50 m) at the top of the carbonate platforms. Around the Gargano Peninsula,

carbonate formations are either associated with Langhian-Tortonian formation (Figure 6a, Branzino borehole located on the Apulian Platform) or Aquitanian-Burdigalian formation (Figure 6a, Cigno Mare). The associated sedimentary hiatuses could either be the result of (i) uplift or subsidence linked to the development of new tectonic phases along the deformation fronts and/or (ii) emersion of the area related to tectonic and relative low sea level.. Conformable Aquitanian-Tortonian marls and carbonates with an average thickness of 150-200m exist at the foot of the slope of the Apulian Platform. Along the SAB, the Aquitanian-Tortonian megasequence fills the Mesozoic Ionian domain with a 900-m-thick depocenter (i.e. Sparviero bis, Figure 6a). In detail, the northern area of the MFS shows an Aquitanian-Burdigalian depocenter with carbonate to silt lateral transition (Figure 6a), whereas the southern area shows a Serravallian-Tortonian depocenter (Figure 6b). A Langhian to Piacenzian hiatus and an erosive unconformity mark the area east of the Gargano Peninsula (Figure 6a – Cigno Mare) and could indicate emersion during this time span.

3. Development of the Messinian syn-MSC megasequence

From the seismic and borehole observation, at least four seismic units were identified offshore across the CAB and SAB (Table 2)

4. The Central Adriatic Basin

The CAB domain in associated to two thin seismic unit named M1 and M2. The M1 Unit can be defined by its seismic facies and its lithological composition, whereas the M2 Unit unit was described from borehole sections only (Figure 6a).

The M1-M2 unit is defined coherently in the western side of the CAB by two continuous seismic reflection of high amplitude and low frequency. The thickness of the unit is homogeneous (0.1 s twt thick about 60 m thickness) and develops locally between the Triassic salt anticlines composing the MAR along the CAB (0.2 s twt thick; Figure 7 – SONE03). This facies was not observed on the eastern part of the CAB and east of the MAR, perhaps due to a different depositional environment and/or to post-Messinian polygenic erosive and wave-cut surfaces (Figure 7 – SONE03-04-06). From a lithological point of view (Figure 6a, 6b), M1 shows a basal clayey carbonate and marl formation (close to the Italian coastline) (Figure 6b –Silvana 001). This succession is conformably covered by gypsiferous beds alternating with either clay or carbonate levels and associated with the PLG (see Manzi *et al.*, 2020 for a review). In some boreholes, the PLG are conformably covered by a 10-m-thick section of clayey carbonate named in this study as

418 the M2 Unit. Along the central part of the CAB, the Messinian units are cut by an erosive surface
419 (Figures 6a, 6b, 7), locally marked by a strong V-shaped incisions (Figure 7 – NOSE03) suggesting
420 a subaerial origin. At least three east-west oriented incised valley systems were observed (Figure
421 5), but their origins as well as their terminations could not be determined mainly due to the
422 scarcity of seismic coverage in this study. According to our observations, the M1 and M2 units
423 do not appear connected with the other MSC deposits identified along the SAB (Figure 5; Figure
424 7 – SONE07; Manzi *et al.*, 2020).

425 **5. The South Adriatic Basin**

426 **The SAB domain** is characterized by two main MSC units (Figure 5) named M3 and M4,
427 and delimited by three erosional discontinuities S20, S22 and S30 (Table 2) which laterally evolve
428 into conformable surfaces toward the eastern part of the SAB (Figure 8 – NOSE04-05). These
429 units can be distinguished from the underlying formations by their seismic facies, their internal
430 geometries and the boundary surfaces.

431 Lithological observations are available for the Sparviero-bis borehole (Figure 6a, 6b), which
432 reaches the upper part of M3: In this area M3 lies on the Messinian Di Letto Fm. (~100m)
433 composed of sandy clay. The upper part of M3 may be associated with the Gessoso-solfifera
434 formation (about 70 m thick), here composed of alternating sandy-clay levels and reworked
435 evaporites. Gamma Ray and Sonic logs (Sparviero bis; Rovesti 001) suggest a detrital origin for
436 this formation instead of an in-situ evaporitic deposition as for the PLG (this study; Manzi *et al.*,
437 2020).

438 The base of M3 Unit is defined by an erosional surface of variable magnitude but traceable at the
439 scale of the entire SAB. The development of the M3 Unit is delineated south of the MFS, on the
440 northern edge of the Tremiti-MAR structure and is delimited south and north by the platform
441 edge of the Apulian and Adriatic platforms (Figure 5). The Mattinata and MAR structures affect
442 the morphology of the basal surface (Figure 8, SONE09: km 20-70), which form a high relief
443 compared to the SAB basin. M3 shows a different seismic facies between the high MFS-MAR
444 structure and the deeper domains, as well as lateral facies evolution towards the southern SAB
445 domain (Figure 9).

446 Southwest of the Mattinata system, M3 is characterized by poor-continuity reflections of medium
447 amplitude and medium frequency (Figure 8 – NOSE02: km 35-50; Supplementary material 2;
448 Figure 9). A fan geometry can be seen in secondary fault systems. This seismic facies evolves

laterally into a chaotic seismic facies with numerous diffraction hyperboles following a SW-NE axis, interpreted as a clastic mass transport deposit (MTD) (Figure 5; Figure 8; Figure 9). The detrital sediments, likely charged in gas, obscure the base of the unit and the underlying formations. The development of the MTD facies limits monitoring of the basal erosional unconformity, thus a maximum thickness of 0.6 s twt is proposed for M3 (Figure 8 – NOSE02). Its thickness is variable and estimated towards the north at 0.3 s twt, which suggests derivation from the Apulian Platform edge.

The unit shows gradual seismic facies change towards the SE with the development of more continuous and sub-parallel reflections (Figure 8 - NOSE02-SONE10; Figure 9). It is worth noting the presence of a pre-Messinian prograding facies developing at the same place as the pre-MSC progradations (Figure 8, NOSE02: km 30-60). In the deep domain of the SAB (Figure 7, SONE07: km 65-120), the edges are also associated with the development of forced regression prisms, with an average thickness of 0.2 s twt (Figure 8, SONE08: km 100-115; SONE09: km130-150).

Along the northern part of the SAB, the top of M3 (S22) is a discontinuity truncating the reflectors of M3, as well as the Aquitanian-Tortonian series where syn-MSC seismic units are absent. The surface becomes concordant towards the SE and underlines the roof of M3. Locally, V-shaped incised valley axes are observed (Figure 8, SONE08: km 123-135; Figure 8, NOSE06: km 95-108), probably related to a NW-SE valley axis developing along the Mesozoic carbonate platform. The origin of the incised valley observed along the CAB remains difficult to define (Figure 5).

M4 Unit is underlain by the S22 discontinuity and is characterized by continuous reflections towards the SE, of high amplitude and medium frequency. The unit also expands towards the SE of the SAB, with more than 0.2 s twt thickness, and fills the depressions at the top of the M3 detrital unit (Figure 8 - NOSE02: km60-168 - NOSE04: km 60-148). Note that prograding reflections develop along a NE-SW axis, within the old incised valley (Figure 8 - NOSE07: km 30-40; SONE09: km 105-120). Basinward, the seismic reflections of M4 become parallel to M3, but we could not estimate the evolution of its thickness towards the Albanid front and the Otranto Strait. Although, due to the lack of information from borehole data, we are unable to provide a direct age for its deposition, M4 corresponds to the development of a

transgressive unit and could be correlated to the Upper Evaporites (DSDP 372: Hsü *et al.*, 1978; Lofi *et al.*, 2011; Roveri *et al.*, 2014) observed in the Western and Central Mediterranean basins.

Discussion

1. Evolution of marine corridors across the Adria plate during the Messinian (7.2 – 5.33 Ma)

The identification of the Gargano-Pelagosa strait and its impact on the distribution of MSC deposits makes it possible to draw detailed palaeotectonic-paleoenvironmental reconstructions of the study area of the Pelagosa Strait during Messinian times (Figures 10-15). For each stage, two maps show the palinspatic reconstruction and palaeoenvironmental information of the area. The kinematic motion of the Calabria block, the Adria plate, and the north Apulian block relative to the Corsica-Sardinia blocks (used as the fixed reference) were restored using Placa4D software (Matias *et al.*, 2005). Figures 10 to 15 illustrate the palinspastic evolution of the study area at 7.2, 5.9, 5.5, 5.36 and 5.3 Ma. Figure 10a (7.2 Ma) corresponds to the transition between rifting and drifting in the future central Tyrrhenian domain (Lymer *et al.*, 2018) which also marks a new compressive phase along the Apennine belt (Vezzani *et al.*, 2010; Ghielmi *et al.*, 2010, 2013).

Following Carminati *et al.* (2012) and Argnani *et al.* (2014), we rotated the Calabria-Peloritani block east of Sardinia and the north Gargano micro-block; however, these authors did not provide angles for the rotation. To be coherent with the geological and geophysical intraplate information, we applied an angle of -8.7° (Table 3) for the Calabria-Peloritain block for a total displacement of 450 km from 7.2 to 0Ma We also took into account a 10°ccw rotation of the Albanid-Hellenide chain with a rotation point located at the Scutari-Pec lineament (van Hinsbergen *et al.*, 2004).

A second constraint comes from the restoration of the limit of the Adria plate and the situation of the Mesozoic Adriatic, Apulia, and Apennine platforms. Palaeomagnetic data from the Apennine Platform show a ~60°ccw rotation (Gattacceca and Speranza, 2002) and constraints from thrust-top sedimentary basins overlying the Southern Apennine chain show ~40ccw rotation in the late Miocene (van Hinsbergen *et al.*, 2020). We elected a ~45 ccw rotation of the Apennine Platform with respect to the Apulian Platform (van Hinsbergen *et al.* (2020) (Figure 10). As suggested by Vezzani *et al.* (2010) and Vitale and Ciarcia (2013), the Apennine and Apulian platforms are connected by a slope domain (Figure 10). This restoration implies a

509 ~200 km wide Sannio-Molise-Lagonegro Mesozoic basin system at the junction with the Ionian
510 Sea. Argnani *et al.* (2009) also suggested that along the MFS compressional deformation
511 dominated since the late Miocene, contributing to create the topographic elevation of the
512 Gargano promontory. According to Tondi *et al.* (2005), dextral component of motion is
513 compatible with the present-day stress field that could be active since the last 200 kyr at rates of
514 0.8+/- 0.1 mm/yr (0.8+/-0.1 km/Myr). According to these results and assuming constant motion
515 during the Pliocene, total displacement of the deep Mesozoic domain north and south of the
516 Mattinata fault system would not exceed 10 km from the late Messinian to Present.

517 The palaeoenvironmental maps are based on these palinspastic constraints and the
518 information on the Messinian sedimentary deposits described in the previous sections.
519 Bathymetry ranges are proposed according to the sedimentary domain, (shelves: 0-200 m; slopes:
520 200-2,000 m; basins and deep domain: 2,000-4,000 m). These values represent average estimates,
521 as does the exact position of the coastline within areas of low constraint due to poor preservation
522 of sedimentary deposits, such as the southern part of the future South Apennine Chain or along
523 the Otranto corridor.

524 **1. Prior to the onset of the MSC (from 7.2 Ma to 5.9 Ma) (Figure 10-11)**

525 During late Tortonian-early Messinian (Figure 10a) the whole Apennine platform and the
526 Molise-Lagonegro Basin were embodied in the Apennine deformation belt (Vezzani *et al.*, 2010;
527 Vitale and Ciarcia, 2013) (. Flysch deposition is recorded on the Apennine Platform (Anversa
528 flysch; Figure 3) and along its eastern border on the Sannio-Molise Basin (Agnone flysch) (Figure
529 3; Vezzani *et al.*, 2010). Calcarenite deposition along the western border of the Apulian Platform
530 (Figure 3) marks the initiation of its deformation (Vezzani *et al.*, 2010). During this period the
531 Laga Basin developed northeast of the deformed Apennine Platform (Milli *et al.*, 2006, 2007)
532 (Figure 10a) which is part of the Marnoso-arenacea-Bolognano flexural basin (e.g. Roveri *et al.*,
533 2003; Milli *et al.*, 2006, 2007; Artoni, 2013). This end-Tortonian deformation phase subdivides
534 the Apennine foredeep into more confined basins with the Po, Romagna, and Laga basins, and
535 records the turbiditic sandstone and mudstone formation of Bagnolo Fm. and Laga Fm. (Table
536 01; Artoni, 2003; Ghielmi *et al.*, 2010) on top of the Serravallian-Tortonian foreland ramp.
537 Associated with this tectonic phase, the inner part of the outer Marnoso-arenacea foredeep is
538 involved in the fold-and-thrust belt (Ricci Lucchi, 1986).

539 This deformation phase also impacted the SE border of the Adria plate during the Messinian to
540 present-day (Figures 10a-15a; Frasheri *et al.*, 2009; van Hinsbergen *et al.*, 2020), with the
541 reactivation and uplift of the Albanid fold-and-thrust belt (Frasheri *et al.*, 1996, 2009), south of
542 the Scutari-Pec lineament. Accordingly, this deformation involved the SE terminal part of the
543 Apulian Platform, thus implying bending towards the south of the eastern part of the Apulian
544 Platform. According to Argnani *et al.* (2009), these late Miocene tectonic phases are associated
545 with a change in tectonic style along the Mattinata fault system, from normal and left-lateral
546 strike-slip motion to compressive dextral strike-slip motion (Figures 10a, 11a).

547 Therefore, prior to the initiation of the MSC (Figure 10b), the Apulian Platform was an
548 island respectively bordered east and west by the Gargano-Pelagosa, Lagonegro and Otranto
549 straits. Both marine corridors delimitate the Messinian Apennine foredeep system from the
550 deeper environmental domains (Figure 10b; Pellen *et al.*, 2017; Manzi *et al.*, 2020). At that time,
551 the Gargano-Pelagosa Strait developed wackestone and argillaceous deposits (Schlier Fm.;
552 Famoso001 borehole) suggesting a shallow to medium water depth (Figure 10b). Several
553 sedimentary hiatuses and traces of erosion are associated with this corridor, suggesting that the
554 Gargano Strait was shallow throughout the Cenozoic era (Patacca *et al.*, 2008) with periods of
555 emersions. This palaeogeographic configuration could be linked to 1) the uplift of the Apulian
556 Platform during Mesozoic and Cenozoic times associated with the Mattinata, Tremiti, and MAR
557 systems, and 3) the uplift of the western part of the Adriatic Platform domain with the influence
558 of the Dinarid-Albanid chains.

559 During late Tortonian-early Messinian time, the western border of the Molise-Lagonegro Basin
560 was progressively affected by the eastward propagation of the Apennine fold-and-thrust belt and
561 foredeep development (Agnone Fm.). According to the tectono-stratigraphic compilation of
562 Ciarcia and Vitale (2013), from 7.2 Ma to 5.9 Ma, the Lagonegro-Molise domain was largely
563 incorporated in the allochthonous tectonic wedge (Figures 10b-11b). The Lagonegro-Molise Strait
564 is therefore interpreted as a shallow marine corridor during the MSC where the depocenters are
565 occurring in a wedge-top or foreland setting.

566 Lastly, the Otranto Strait width remains hypothetic and dependent on the Albanid thrust-front
567 propagation. For our reconstruction, we chose the Mesozoic palaeogeogeographic domain
568 observed along the Albanid fold-and-thrust belt (the Sazani Platform domain (location Figure 3)
569 associated with the Apulian Platform and the Ionian domain associated with the SAB). In this

reconstruction (Figure 10b), the Otranto Strait brings the SAB and the Ionian Sea into contact. It is locked to the west by the Apulian Platform and to the east by the Albanid-Hellenide fold-and-thrust belt. The Messinian to Pliocene tectonic phases affecting this chain may have progressively limited the sedimentary transfer from the SAB toward the Ionian Sea.

2. First stage of the MSC (from 5.97 Ma to 5.6 Ma) (Figures 11-12)

The onset of the Messinian Salinity Crisis with a drastic reduction in the marine connection between the Mediterranean Sea and the Atlantic Ocean at 5.97 Ma (Manzi *et al.*, 2013). At this time, the Apenninic foreland was a shallow evaporitic marine domain (PLG Fm.; Lugli *et al.*, 2010; Manzi *et al.*, 2020) with an average palaeo-water depth not exceeding 200 m (Figure 11b). It then evolves towards the deeper part into organic-rich barren shale (Manzi *et al.*, 2007). The Laga and Romagna basins formed the main foredeep depocenter with at least 2.5-km-thick turbiditic deposition between 7.2 and 5.6 Ma (Milli *et al.*, 2007), associated with sediment sources related to the Apennine Chain and the Alps following a N-S palaeocurrent and NW-SE paleocurrent direction (Milli *et al.*, 2007). This depocenter was limited to the south by 1) the uplift of the former Apennine domain, now embedded in the allochthonous tectonic wedge, 2) the uplift of the Gargano-Pelagosa Strait, and 3) possible tectonic inversion along the MAR and MFS (Figure 11a). This substantial uplift of the area could be related to the opposing compressive reactivation of the Albanid and Apennine Chains (Fantoni and Franciosi, 2010) and/or the inversion of the MFS (Argnani *et al.*, 2009). This motion may have led to a restriction of the Gargano-Pelagosa Strait during stage 1 (Figures 11b, 12b), and/or even to outright marine closure between 5.97 and 5.6 Ma, as no PLG Fm. has been observed along the strait.

Narrow marine corridors could have existed along the former Molise-Lagonegro Strait during stage 1, bordered to the west and east by the Apennine front propagation and the Apulian Platform. The presence of decameter-sized PLG blocks on present-day wedge-top basin outcrops along the south Apennine Chain (Figure 16; Matano, 2007; Matano *et al.*, 2014; Manzi *et al.*, 2020) confirms the deposition of shallow evaporitic formations along the deformation front and/or on the Apulian foreland area. Along the Apennine foredeep, evaporitic deposits of this period are interbedded with marine clays, indicating marine incursions into the shallow basins and reconnection of the Mediterranean, as mainly evidenced by fish remains (Sturani, 1973; Fontes *et al.*, 1987; Carnevale *et al.*, 2008) and dinoflagellate cysts (Bertini, 2006).

3. Second MSC stage (from 5.6 Ma to 5.55 Ma) (Figures 12-13)

The major Mediterranean Sea level drawdown that characterized the paroxysmal step of the MSC occurred at 5.6 Ma (Clauzon *et al.*, 1996, 1997; Bache *et al.*, 2012, 2015; Gorini *et al.*, 2015). This period also corresponds to a new deformation phase recorded throughout the central Mediterranean area and particularly along the Apennine fold-and-thrust belt (Figure 3; Vezzani *et al.*, 2010; Milli *et al.*, 2007; Roveri *et al.*, 2008). The activation of several thrust fronts along the Apennine fold-and-thrust belt as well as on the southern border of the Laga Basin led to incorporate the Messinian foredeep in the belt and initiated a late Messinian-early Pliocene foredeep (Figure 3; Figures 12a-13a; Milli *et al.*, 2007; Vezzani *et al.*, 2010; Artoni, 2012).

Several observations attest to a total disconnection of the Apennine foredeep with respect to the SAB or the Ionian Sea. The marginal domains and thrust-top basins are affected by a subaerial erosional surface; the deeper domains and foredeeps are associated with the development of gypsum-rich turbidites resulting from the erosion of the PLG. The occurrence of an incised-valley system on the foreland part (Figure 13b) confirms a relative sea-level fall comprised between 200 and 800 m, following the flexural back-stripping results modelled by Amadori *et al.* (2018). This relative sea-level fall estimate differs depending of the studied area (marginal basin connected or disconnected to the deeper basins; the hydrogeological and climatic system), where higher estimates of relative sea-level fall have been inferred for the western and eastern Mediterranean (~1000-1500 m) through stratigraphic observation and backstripping modelling (Leroux *et al.*, 2017; Ben-Moshe *et al.*, 2020; Pellen *et al.*, 2019). Freshwater, probably supplied in abundance by the surrounding uplands (Alps: Fauquette *et al.*, 2015a; Apennines: Fauquette *et al.*, 2015b), filled the Apennine foredeep and Po Basin where relatively high water levels persisted during the lowered Mediterranean Sea level in subaqueous brackish environments (Lago Mare biofacies; Gillet, 1968; Colalongo *et al.*, 1976; Bellagamba, 1978; Corselli and Grecchi, 1984; Esu and Taviani, 1989; Faranda *et al.*, 2007; Gliozzi *et al.*, 2007; Popescu *et al.*, 2007; Esu, 2007; Bache *et al.*, 2012; Pellen *et al.*, 2017) (Figure 13b).

At 5.6 Ma, the western side of the Apulian Platform edge was overthrust by the tectonic prism of the southern Apennine Chain (Figures 12a, 13a; Barone *et al.*, 2006; Matano, 2007; Vezzani *et al.*, 2010; Matano *et al.*, 2014). The southern Apennines experienced a strong tectonic phase as attested by syn-tectonic thrusting during the deposition of RLG and after the erosion of PLG (Figure 16; Matano, 2007). This mass transport complex includes pluri-decameter PLG

blocks which suggest a close source of erosion and resettlement in the nearby narrow and shallow environment. Important wedge uplifts were recorded by apatite fission-track data (cooling ages clustering around 5.5 Ma; Corrado *et al.*, 2005; Mazzoli *et al.*, 2008; Ascione *et al.*, 2012), which suggest important horizontal and vertical motions from late Messinian to the present. Along the Apulian foreland, the RLG deposits are also specific to the footwall of normal faults associated with the Mesozoic extensional phase along the Apulian Platform (Manzi *et al.*, 2020). Along the western side of the Apulian foreland, breccia, erosive surface or conglomerate deposits are observed in boreholes, overlain by early Pliocene marls (Figure 5; Pellen, 2016; Manzi *et al.*, 2020). These different observations suggest a relative sea level drop either linked to a sea level fall and/or a tectonic uplift. A different sedimentary history is preserved along the present-day south Apennine chain compared to the CAB and central Apennine chain. These different observations suggest a complete disconnection between the Messinian Apenninic foredeep and the deep Ionian Sea during the MSC paroxysm across the Molise-Lagonegro Strait or the Gargano-Pelagosa Strait.

Along the SAB, the MSC paroxysm is associated with the development of a mass transport deposit, embedded in the M3 seismic unit. The latter includes resedimented clastic gypsum (Figure 6b – Sparviero bis borehole), which indicates the erosion and re-sedimentation of primary evaporites. A possible origin of this MTD could be associated with the eastern Apulian Platform edge and is synchronous with the development of M3 detrital unit during the MSC paroxysm. As there is no major MSC fluvial system located west of the Apulian platform, a possible origin for the MTD could be linked to slope destabilization and submarine landslide. Third MSC stage (from 5.55 Ma to 5.33 Ma) (Figures 13-15).

An age of 5.46 Ma has been proposed for the marine reflooding of the Mediterranean (Bache *et al.*, 2012, 2015; Gorini *et al.*, 2015; Popescu *et al.*, 2021). However, marine waters did not immediately enter the Apennine foredeeps because the marine ingression in such domain, corresponding to the boundary between the p-ev1 and p-ev2 formations (see Table 1; Popescu *et al.*, 2007), has been precisely dated at 5.36 Ma (Bache *et al.*, 2012). From 5.36 Ma (Figure 14b), marine waters overflowed the paleobarrier made by the Gargano-Pelagosa gateway and penetrated the Apennine foredeep composed of brakish water from Paratethyan origin (the third Lago Mare biofacies in Popescu *et al.*, 2015). At least four overflows of marinewaters have been suggested (Pellen *et al.*, 2017), which possibly later flooded the Po Basin (Channell *et al.*, 1994; Sprovieri *et al.*, 2008; Violanti *et al.*, 2011). From a brakish environment, this process was probably forced,

first by the isostatic response of the palaeo-barrier linked to the Apennine deformation phase and/or to the reflooding of the Mediterranean Basin, and then by the continuous global sea-level rise after 5.33 Ma (Figure 15b; Gorini *et al.*, 2015).

Three Lago Mare events have been distinguished and documented in the Mediterranean Basin by Do Couto *et al.* (2014) and Popescu *et al.* (2015) but Roveri *et al.* (2014) considered only one Lago Mare event on the basis of the Apennine foredeep data where only the third Lago Mare event occurred (Pellen *et al.*, 2017). In a recent synthesis on this biofacies, Andreetto *et al.* (2021a) surprisingly followed the model of one Lago Mare event for the whole Mediterranean Basin although they confirmed the marine context of Lago Mare 1 and 3 (Andreetto *et al.*, 2021b) consistently with Do Couto *et al.* (2014), Clauzon *et al.* (2015), and Popescu *et al.* (2015).

After 5.3 Ma and the marine reflooding of the Bradanic and Apennine foredeeps, two more tectonic phases were recorded along the Apennine fold-and-thrust belt (Figure 3): Early-Middle Pliocene and Late Pliocene-Early Pleistocene (Vezzani *et al.*, 2010; Artoni, 2013; Ascione *et al.*, 2012; Vitale and Ciarcia, 2013). These tectonic phases led to the inclusion of the Laga Basin and other Messinian foredeep systems in the fold-and-thrust belt. The total estimated shortening along the central Apennine Chain is estimated between 13 km (L.S to A.A. lineaments) and 32 km (A.A. to M.R. lineaments) (Artoni, 2013; see Figure 2 for the location of lineaments), depending on the segment affected by the deformation. Along the Southern Apennine, the Apennine allochthonous wedge continued to be thrusted over the Apulian Platform (Mazzoli *et al.*, 2008). Active thrusting migrated to the underlying platform during the Pliocene, and was accompanied by a switch from thin-skinned thrusting to thick-skinned inversion-dominated shortening (Mazzoli *et al.*, 2000; Butler and Mazzoli, 2006; Shiner *et al.*, 2004; Ascione *et al.*, 2012). From 5.3 Ma to the present, the migration of the allochthonous tectonic wedge has been estimated between 50 and 60 km (Ascione *et al.*, 2012).

2. Intra-Messinian isostatic rebound and platform destabilization

Neogene horizontal and vertical motion changes should have affected the morphology of the Gargano-Pelagosa gateway as well as the SAB: the MAR and MFS seem to delimitate the SAB into two sub-basins following a NW-SE axis (Figure 8). The eastern part of the basin has thicker Paleogene-Miocene, Messinian, and Pliocene-Quaternary sedimentary successions compared to the western sub-basin.

The distribution of the different MSC-related formations around the Gargano-Pelagosa strait provides cogent constraints on the palaeoenvironmental and tectonic evolution along the Adria plate (Figures 5, 11-15). Moreover, the development of the MTD (M3 seismic unit) – originated from the Apulian platform edge – could be associated to several tectonic and/or eustatic processes affecting the area.

Similar MSC deposits have been recognized along the Mediterranean: the Valencia-Menorca basins (Maillard *et al.*, 2006; Cameselle and Urgeles, 2016; Pellen *et al.*, 2019), the Alboran Sea (del Olmo and Comas, 2008; del Olmo, 2011), the Malta Escarpment (Micallef *et al.*, 2018; Garcia-Castellanos *et al.*, 2020). MTDs have been associated with various processes (Canals *et al.*, 2004; Moscardelli and Wood, 2007) in the case of the Messinian event. Their origin is associated with seismotectonic activity and/or strong sea-level fluctuation and marine gas-hydrates release, isostatic rebound, and adaptation of river equilibrium profiles. In view of their stratigraphic position in the Alboran and Valencia basins, the emplacement of the MTDs was dated at around 5.60 Ma as a consequence of the sea-level fall and ensuing isostatic rebound of the continental shelves (del Olmo and Comas, 2008; Pellen *et al.*, 2019). The development of MTDs along the Maltese Escarpment was associated with the rapid sea-level rise at the end of the MSC (Garcia-Castellanos, 2009; Micallef *et al.*, 2018), but a tectonic origin linked to the destabilisation of the platform cannot be ruled out. Modelling of isostatic rebound only linked to the withdrawal of water masses around the Gargano-Pelagosa Strait suggests isostatic uplift values between 200 and 1000 m (DeCelles and Cavazza, 1995; Cavazza and DeCelles, 1998; Gargani et al, 2010; Amadori *et al.*, 2018). This wide range is dependent on the palaeogeography and the nature of the associated basins and landforms (Govers *et al.*, 2009) as well as the tectonic setting, and reflects the important vertical movements affecting the Mediterranean marginal domains. More than 1.3 km were measured on the Gulf of Lion margin for the MSC period and associated with water withdrawal and large sediment transfers (Rabineau *et al.*, 2014).

Major tectonic re-organization are documented along the Adria plate during the MSC: (1) the intra-Messinian tectonic phase impact the whole Apennine chain (see Discussion 1.3) and Albanid chain (e.g. Pashko and Aliaj, 2020); (2) change from sinistral to dextral strike-slip motion and folding along the MFS have been documented for the late Miocene (Argnani *et al.*, 2009). Together with the abrupt changes in sea level, these tectonic processes are perfect candidates to explain the establishment of the MTD (M3 unit) in the SAB.

At a regional scale other major tectonic change (Giaconia *et al.*, 2018) and major magmatic pulse (Sternai *et al.*, 2017) are observed. These Mediterranean tectonic/magmatic pulses have been also linked to a more global plate kinematic reorganization affecting the earth during Messinian time (Leroux *et al.*, 2018). These changes in horizontal motion also affect the submarine morphology and kilometer scale uplift have been documented world-wide (Rabineau *et al.*, 2014; Masters *et al.*, 2020). As highlighted by Booth-Rea *et al.* (2018) or Masters *et al.* (2020), these uplift affecting the gateways favoured the faunal and floral migration between continents. The episodic emergence of the Gargano-Pelagosa gateway during the MSC, and more generally during the Mesozoic and Cenozoic, could also explain the faunal migration between the different Mesozoic platforms of the former Greater Adria plate (Zarcone *et al.*, 2010; van Hinsbergen *et al.*, 2020).

Conclusions

The Gargano-Pelagosa gateway is here first recognized as an influential element of the palaeogeographic/environmental evolution of the central-southern Apenninic foredeep and wedge-top domains during the Messinian, as shown by the integration of (i) seismic lines, (ii) well information from the Adriatic Sea, and (iii) a review of both onshore and offshore structural data and Messinian depositional environments. Several processes concur to explain the isolation of the Apennine foredeep during the MSC. Primarily, NW-SE oriented Mesozoic platforms and basins systems controlled the Neogene sedimentary environments around the Gargano-Pelagosa Strait. Messinian tectonic rejuvenation along the Apenninic and Albanid fold-and-thrust belts, the Mid-Adriatic Ridge and Mattinata Fault System, led to the isolation of the Apennine foredeep during the MSC paroxysm. We propose a coherent tectonic and environmental evolution along the Adria plate during the MSC:

1. During MSC stage 1, the CAB evolved into a large evaporitic basin (Manzi *et al.*, 2020) only connected to the deep Mediterranean basins east and west of the Apulian Platform through the Gargano-Pelagosa and Lagonegro straits, respectively.
2. During the initiation of the stage 2, the combined effects of the MSC sea-level fall and the ensuing intra-Messinian tectonic rejuvenation along the Apennine Chain led to the closure of the Lagonegro Strait. We suggest that the widespread deposition of mass transport deposits across the SAB is related to the isostatic rebound along the Apulian Platform. Tectonic inversion of the Mattinata Fault System could also be associated with

intra-Messinian tectonics. These multiple tectonic processes led to the closure of the Gargano-Pelagosa Strait and isolation of the Apennine foredeep, as suggested by Pellen *et al.* (2017) and Manzi *et al.* (2020).

In the same way, the Otranto Strait could have been also influenced during the MSC by the isostatic rebound related to sea-level fall and sedimentary transfer, and by tectonic deformation along the Albanid-Peloponnese fold-and-thrust belt. Further seismic and borehole investigation could highlight the sedimentary relationship between the SAB and the Ionian Sea.

Acknowledgment

We acknowledge the "Visibilità dei dati afferenti all' atticità du esplorazione petrolifera in Italia (VIDEPI)" for the public release of borehole and seismic data and their easy access. This work was supported by Action Marge project, Labex MER and the ISblue Theme 2 project, co-funded by a post-doctoral grant awarded to R. Pellen by IFREMER and UBO. We are also grateful to Alison Chalm for English proofreading.

Conflict of interest

We confirm that we have no conflicts of interest related to this research, this work is original to its form and has not been published elsewhere, nor is under consideration for publication elsewhere.

Bibliography

Afilhado, A., Moulin, M., Aslanian, D., Schnürle, P., Klingelhoefer, F., Nouzé, H., Rabineau, M., Leroux, E., and Beslier, M.-O., 2015, Deep crustal structure across a young passive margin from wide-angle and reflection seismic data (The SARDINIA Experiment) – II. Sardinia's margin: Bulletin de la société géologique de france, v. 186, p. 331-351.

Amadori, C., Garcia-Castellanos, D., Toscani, G., Sternai, P., Fantoni, R., Ghielmi, M., and Di Giulio, A., 2018, Restored topography of the Po Plain-Northern Adriatic region during the Messinian base-level drop—Implications for the physiography and compartmentalization of the palaeo-Mediterranean basin: Basin Research, p. 1-17.

Amore, O., Ciampo, G., Ruggiero, E., Santo, A., and Sgrasso, I., 1988, La successione miocenica del Matese nord-occidentale: nuevi dati biostratigrafici e conseguenti ipotesi paleogeografiche: Memorie della Societa Geologica d'Italia, v. 41, p. 311-319.

Andreetto, F., Aloisi, G., Raad, F., Heida, H., Flecker, R., Agiadi, K., Lofi, J., BLondel, S., Bulian, F., Camerlenghi, A., Caruso, A., Ebner, R., Garcia-Castellanos, D., Gaullier, V., Guibourdenche, L., Gvirtzman, Z., Hoyle, T.M., Meijer, P.T., Moneron, J., Sierro, F.J., Travan, G., Tzevahirtzian, A., Vasiliev, I., and Krijgsman, W., 2021a, Freshening of the Mediterranean Salt Giant: controversies and certainties around the terminal (Upper Gypsum and Lago-Mare) phases of the Messinian Salinity Crisis: Earth-Science Reviews, v. 216, 103577.

Andreetto, F., Matsubara, K., Beets, C.J., Fortuin, A.R., Flecker, R., and Krijgsman, W., 2021b. High Mediterranean water-level during the Lago-Mare phase of the Messinian Salinity Crisis: insights from the Sr isotope records of Spanish marginal basins (SE Spain). Palaeogeography, Palaeoclimatology, Palaeoecology, v. 562, 110139.

Andriani, G.F., Walsh, N., and Pagliarulo, R., 2005, The influence of the geological setting on the morphogenetic evolution of the Tremiti Archipelago (Apulia, Southeastern Italy): Natural Hazards and Earth System Sciences, v. 5, p. 29-41.

Argnani, A., 2013, The influence of Mesozoic palaeogeography on the variations in structural style along the front of the Albanid thrust-and-fold belt: Italian Journal of Geosciences, v. 132, p. 175-185.

Argnani, A., 2014, Mesozoic palaeogeography of Adria: Hints on the origin of the Skutari-Pec Line: In: Beqiraj., A., Ionescu, C., Christofides, G., Uta, A., Beqiraj, Goga, E., Marku, S. (Eds.). Proceedings of XX CBGA Congress of the Carpathian-Balkan Geological Association, Tirana (Albania). Special session of the Buletini i Shkencave Gjeologjike, v. 1, p. 120

Argnani, A., Favali, P., Frugoni, F., Gasperini, M., Ligi, M., Marani, M., Mattietti, G., and Mele, G., 1993, Foreland deformational pattern in the Southern Adriatic Sea: Annales Geophysicae, v. 36, p. 229-247.

Argnani, A., and Gamberi, F., 1995, Stili strutturali al fronte della catena appenninica nell'Adriatico centro-settentrionale: Studi Geologici Camerti Special volume, v. 1, p. 19-27.

Argnani, A., Rovere, M., and Bonazzi, C., 2009, Tectonics of the Mattinata fault, offshore south Gargano (southern Adriatic Sea, Italy): Implications for active deformation and seismotectonics in the foreland of the Southern Apennines: Geological Society of America Bulletin, v. 121, p. 1421-1440.

Artoni, A., 1993, Modello sedimentario e di flessurazione di un tratto del margine adriatico in un settore dell' Appennino Centrale: Ph.D. thesis - Universita' di Parma, p. 301 p.

Artoni, A., and Casero, P., 1997, Sequential balancing of growth structures, the late tertiary example from the central Apennine: Bulletin de la société géologique de france, v. 168, p. 35-49.

Artoni, A., 2013, The Pliocene-Pleistocene stratigraphic and tectonic evolution of the Central sector of the Western Periadriatic Basin of Italy: Marine and Petroleum Geology, v. 42, p. 82-106.

Ascione, A., Ciarcia, S., Di Donato, V., Mazzoli, S., and Vitale, S., 2012, The Pliocene–Quaternary wedge-top basins of southern Italy: an expression of propagating lateral slab tear beneath the Apennines: Basin Research, v. 24, p. 456–474.

Bache, F., Olivet, J.-L., Gorini, C., Rabineau, M., Baztan, J., Aslanian, D., and Suc, J.-P., 2009, Messinian erosional and salinity crises: view from the provence basin (Gulf of Lions, Western Mediterranean). : Earth and Planetary Science Letters, v. 286, p. 139-157.

827 Bache, F., Popescu S.M., Rabineau, M., Gorini, C., Suc, J.P., Clauzon G., Olivet J-L., Rubino J-L., Melinte-
828 Dobrinescu M.C., Estrada F., Londeix L., Armijo R., Meyer B., Jolivet L., Jouannic G., Leroux
829 E., Aslanian D., Baztan J., Dos Reis A.T., Mocochain L., Dumurdzanov N., Zagorchev I., Lesic
830 V., Tomic D., Cagatay M.N., Brun J-P., Sokoutis D., Csato I., Ucarkus G., and Cakir Z., 2012, A
831 two-step process for the reflooding of the Mediterranean after the Messinian Salinity Crisis: Basin
832 Research, v. 23, p. 1-29.
833 Bache, F., Gargani, J., Suc J.-P., Gorini, C., Rabineau, M., Popescu, S.M., Leroux, E., Do Couto, D.,
834 Jouannic, G., Rubino, J.-L., Olivet, J.-L., Clauzon, G., Dos Reis, A., and Aslanian, D., 2015, Mes-
835 sinian evaporite deposition during sea level rise in the Gulf Of Lions (Western Mediterranean):
836 Marine and Petroleum Geology, v. 66, p. 262-277.
837 Balázs, A., Granjeon, D., Matenco, L., Sztanó, O., and Cloetingh, S., 2017, Tectonic and climatic controls
838 on asymmetric half-graben sedimentation: inferences from 3-D numerical modelling: Tectonics,
839 v. 36, p. 2123-2141.
840 Bally, A.W., Burbi, L., Cooper, C., and Ghelardoni, R., 1986, Balanced sections and seismic reflection
841 profiles across the Central Apennines: Memorie dellà Società Geologica Italiana, v. 35, p. 257-
842 310.
843 Barone, M., Critelli, S., Le Pera, E., Di nocera, S., Matano, F., and Torre, M., 2006, Stratigraphy and
844 Detrital Modes of Upper Messinian Post-evaporitic Sandstones of the Southern Apennines, Italy:
845 Evidence of Foreland-Basin Evolution during the Messinian Mediterranean Salinity Crisis: Inter-
846 national Geology Review, v. 48, p. 702-724.
847 Barone, M., Dominici, R., Muto, F., and Critelli, S., 2008, Detrital modes in a late Miocene wedge-top
848 basin, northeastern Calabria, Italy: compositional record of wedgetop partitioning: Journal of
849 Sedimentary Research, v. 78, p. 693-711.
850 Ben-Moshe, L., Ben-Avraham, Z., Enzel, Y., and Schattner, U., 2020, Estimating drawdown magnitudes
851 of the Mediterranean Sea in the Levant basin during the Lago Mare stage of the Messinian Salinity
852 Crisis: Marine Geology, v. 427.
853 Bellagamba, M., 1978. Gli "strati a Congerie" di Capanne di Bronzo (Pesaro) del Messiniano terminale e
854 deduzioni paleoambientali. Acta Naturalia dell'Ateneo Parmense 14, 207–222.
855 Bertini, A., 2006, The Northern Apennines palynological record as a contribute for the reconstruction of
856 the Messinian palaeoenvironments: Sedimentary geology, v. 78, p. 115-121.
857 Betzler, C., Braga, J.C.,Martin, J.M., Sanchez-Almazo, I.M., Lindhorst, S., 2006, Closure of a seaway: strat-
858 igraphic record and facies (Guadix basin, Southern Spain): Int J Earth Sci.
859 Bigi G., Castellarin A., Coli M., Dal Piaz G.V., Sartori R., Scandone P. & Vai G.B., 1990. *Structural Model*
860 *of Italy scale 1:500.000, sheet 1-6.* C.N.R., Progetto Finalizzato Geodinamica, SELCA Firenze.
861 Bigi, S., Milli, S., Corrado, S., Casero, P., Aldega, L., Botti, F., Moscatelli, M., Stanzione, O., Falcini, F.,
862 Marini, M., and Cannata, D., 2009, Stratigraphy, structural setting and burial history of the Mes-
863 sinian Laga basin in the context of Apennine foreland basin system: Journal of Mediterranean
864 Earth Sciences, v. 1, p. 61-84.
865 Bigi, S., Casero, P., and Ciotoli, G., 2011, Seismic interpretation of the Laga basin; constraints on the
866 structural setting and kinematics of the Central Apennines: Journal of the Geological Society,, v.
867 168, p. 1-11.
868 Billi, A., Gambini, R., Nicolai, C., and Storti, F., 2007, Neogene-Quaternary intraforeland transpression
869 along a Mesozoic platform-basin margin: The Gargano fault system, Adria, Italy: Geosphere, v. 3,
870 p. 1-15.
871 Boccaletti, M., Ciaranfi, N., Cosentino, D., Deiana, G., Gelati, R., Lentini, F., Massari, F., Moratti, G.,
872 Pescatore, T., Ricci Lucchi, F., and Tortorici, L., 1990, Palinspastic restoration and
873 paleogeographic recontruction of the Peri-Tyrrhenian area during the Neogene: palaeogeography,
874 Palaeoclimatology, Palaeoecology, v. 77, p. 41-50.
875 Booth-Rea, G., Ranero, C.R., and Grevemeyer, I., 2018, The Alboran volcanic-arc modulated the Mes-
876 sinian faunal exhange and salinity crisis: Nature Scientific Reports, v. 8, p. 13015.
877 Bosellini, A., 2002, Dinosaurs "re-write" the geodynamics of the eastern Mediterranean and the paleoge-
878 ography of the Apulia Platform: Earth-Science Reviews, v. 59, p. 211-234.

879 Butler, R.W.H., Lickorish, W.H., Grasso, M., Pedley, H.M., and Ramberti, L., 1995, Tectonics and se-
880 quence stratigraphy in Messinian basins, Sicily: Constraints on the initiation and termination of
881 the Mediterranean salinity crisis: Geological Society of America, v. 107, p. 425-439.
882 Butler, R.W.H., and Mazzoli, S., 2006, Styles of continental contraction: a review and introduction: In:
883 Styles of Continental Contraction (Ed. by S. Mazzoli and R.W.H. Butler), GSA Special Paper, v.
884 414, p. 1-10.
885 Butler, R.W.H., Maniscalco, R., and Pinter, P.R., 2019, Syn-kinematic sedimentary systems as constraints
886 on the structural response of thrust belts: re-examining the structural style of the Maghrebian
887 thrust belt of Eastern Sicily: Italian Journal of Geosciences, v. 138.
888 Cameselle, A.L., and Urgeles, R., 2016, Large scale margin collapse during Messinian early sea-level draw-
889 down: the SW Valencia trough, NW Mediterranean: Basin research, v. 29, p. 576-595.
890 Camerlenghi, A., Del Ben, A., Hübscher, C., Forlin, E., Geletti, R., Brancatelli, G., Micallef, A., Saule,
891 M., and Facchin, L., 2020, Seismic markers of the Messinian salinity crisis in the deep Ionian
892 Basin: Basin Research, v. 32, p. 716-738.
893 Canals, M., Casamor, J.L., Lastras, G., Monaco, A., Acosta, J., Berné, S., Loubrieu, B., Weaver, P.P.E.,
894 Grehan, A., and Dennielou, B., 2004, The Role of Canyons in Strata Formation: Oceanography,
895 v. 17, p. 81-91.
896 Carnevale, G., Caputo, D., Landini, W., 2008. A leerfish (Teleostei, Carangidae) from the Messinian
897 evaporite succession of the Vena del Gesso basin (Romagna, Apennines, Italy): palaeogeograph-
898 ical and palaeoecological implications. Bollettino della Societa` Paleontologica Italiana 47, 169–
899 176.
900 Casero, P., 2004, Structural setting of petroleum exploration plays in Italy: Italian Geological Society.
901 Casero, P., and Bigi, S., 2012, Structural setting of the Adriatic basin and the main related petroleum
902 exploration plays: Marine and Petroleum Geology.
903 Carminati, E., Lustrino, M., and Doglioni, C., 2012, Geodynamic evolution of the central and western
904 Mediterranean: Tectonics vs. igneous petrology constraints: Tectonophysics, v. 579, p. 173-192.
905 Cavazza, W., and DeCelles, P.G., 1998, Upper Messinian siliciclastic rocks in southeastern Calabria
906 (southern Italy): palaeotectonic and eustatic implications for the evolution of the central Mediter-
907 ranean region: Tectonophysics, v. 298, p. 223-241.
908 Cavazza, W., Roure, F., Spakman, Stampfli, G.M., and Ziegler, P.A., eds., 2004, The TRANSMED Atlas:
909 the Mediterranean Region from Crust to Mantle: Heidelberg, Springer-Verlag, 141 pp. + CD-
910 ROM.
911 Centamore, E., and Nisio, S., 2003, Significative events in the Periadriatic foredeeps evolution (Abruzzo-
912 Italy). Studi Geologici Camerti, v. num. spec. 2003, p. 39-48.
913 Channell, J.E.T., Catalano, R., and D'Argenio, B., 1980, Paleomagnetism and deformation of the
914 Mesozoic continental margin in Sicily: Tectonophysics, v. 61, p. 391-407.
915 Channell , J.E.T., Poli, M.S., Rio, D., Sprovieri, R., and Villa, G., 1994, Magnetic stratigraphy and bio-
916 stratigraphy of Pliocene "argille azzurre" (Northern Apennines, Italy): Palaeogeography, Palaeocli-
917 matology, Palaeoecology, v. 110, p. 83-102.
918 Ciaranfi, N., Dazzaro, L., Pieri, P., Rapisardi, L., and Sardella, A., 1973, Geologia della zona compresa fra
919 Bisaccia (Av): Memorie della Societa Geologica Italiana, v. 12, p. 279-315.
920 Ciarapica, G., and Passeri, L., 2002, The palaeogeographic duplicity of the Apennines: Bollettino della
921 Società geologica italiana, v. 121, p. 67-75.
922 CIESM, 2008, The Messinian Salinity Crisis from mega-deposits to microbiology- A consensus report:
923 CIESM workshop Monograph [F. Briand, Ed.], v. 33, p. 168p.
924 Cippitelli, G., 2007, The CROP-04 seismic profile. Interpretation and structural setting of the Agropoli-
925 Barletta Geotraverse: Bollettino della Societa Geologica Italiana, v. 7, p. 267-281.
926 Chiocchini, U., Madonna, S., Barbieri, M., Si Stefano, A., Le Pera, E., and Potetti, M., 2003, Le unita
927 tardo orogene dell'area tra Benevento ed Avellino (Appennino Campano): In: Studi Geologici
928 Camerti, numero speciale Edimont, Citta di Castello (PG), p. 49-62.
929 Chorowicz, J., Cadet, J.-P., and Stephan, J.-F., 1981, Le secteur transversal de Scutari-Pec: apports de
930 l'étude de la fracturation à partir des données landsat: Bulletin de la société géologique de france,
931 v. 18, p. 217-228.

Clauzon, G., Rubino, J.-L., and Casero, P., 1997, Regional modalities of the Messinian Salinity Crisis in the framework of a two phases model. : R.C.M.N.S. Interim-Colloquium, Catane, p. 44-46.

Clauzon, G., Suc, J.P., Gautier, F., Berger, A., and Loutre, M.F., 1996, Alternate interpretation of the Messinian salinity crisis: controversy resolved? : Geology, v. 24 p. 363-366.

Clauzon G., Suc J.-P., Do Couto D., Jouannic G., Melinte-Dobrinescu M.C., Jolivet L., Quillévéré F., Lebret N., Mocochain L., Popescu S.-M., Martinell J., Doménech R., Rubino J.-L., Gumiaux C., Warny S., Bellas S.M., Gorini C., Bache F., Rabineau M., and Estrada F., 2015. New insights on the Sorbas Basin (SE Spain): The onshore reference of the Messinian Salinity Crisis. Marine and Petroleum Geology, 66, 71-100.

Colalongo, M.L., Cremonini, G., Farabegoli, E., Sartori, R., Tampieri, R., Tomadin, L., 1976. Palaeoenvironmental study of the ''Colombacci'' Formation in Romagna (Italy): the Cella section. Memorie della Societa` Geological Italiana 16, 197–216.

Corrado, S., Aldega, L., Di Leo, P., Giampaolo, C., Invernizzi, C., Mazzoli, S., and Zattin, M., 2005, Thermal maturity of the axial zone of the southern Apennines fold-and-thrust belt (Italy) from multiple organic and inorganic indicators: Terra Nova, v. 17, p. 56-65.

Corradini, D., and Biffi, U., 1988, Dinocyst study at the Messinian-Pliocene boundary in the Cava Serredi section, Tuscany, Italy: Bulletin des Centres de Recherches Exploration-Production Elf-Aquitaine, v. 12, p. 221-236.

Cosentino, D., Buchwaldt, R., Sampalmieri, G., Ladanza, A., Cipollari, P., Schildgen, T.F., Hinnov, L.A., Ramezani J., and Bowring, S.A., 2013, Refining the Mediterranean "Messinian gap" with high-precision U-Pb zircon geochronology, central and northern Italy: Geology, v. 41, p. 323-326.

Corselli, C., and Grecchi, G., 1984. The passage from hypersaline to hyposaline conditions in the Mediterranean Messinian: discussion of the possible mechanisms triggering the ''Lago Mare'' facies. Pale´ obiologie continentale 14 (2), 225–239.

De Alteriis, G., 1995, Different foreland basins in Italy: examples from the central and southern Adriatic Sea: Tectonophysics, v. 252, p. 349-373.

DeCelles, P., and Cavazza, W., 1995, Upper Messinian fanglomerates in eastern Calabria (southern Italy): response to microplate migration and Mediterranean sea-level changes: Geology, v.23, p.775-778.

Dellong, D., Klingelhoefer, F., Kopp, H., Graindorge, D., Margheriti, L., Moretti, M., Murphy, S., and Gutcher, M.-A., 2018, Crustal structure of the Ionian basin and eastern Sicily margin: Results froma wide-angle seismic survey: Journal of Geophysical Research: Solid Earth, v. 123.

Del Olmo, W.M., 2011, The Messinian in the Gulf of Valencia and Alboran Sea (Spain): paleogeography and paleoceanography implications: Revista de la Sociedad Geológica de España, v. 24, p. 1-22.

Del Olmo, M.W., and Comas, M., 2008, Arquitectura sísmica, olistostromas y fallas extensionales en el norte de la cuenca oeste del mar de Alborán. : Revista de la Sociedad Geológica de España, v. 21, p. 151-167.

Dercourt, J., and Fleury, J.J., 1972, The Canadian Cordilliera, the Hellenides, and the Sea-floor Spreading theory: Canadian Journal of Earth Sciences, v. 9, p. 709-743.

Di Nocera, S., Matano, F., Pescatore, T., Pinto, F., Quarantiello, R., Senatore, M.R., and Torre, M., 2006, Schema deologico del transetto Monti Picentini orientali-Monti della Daunia meridionali: unita stratigrafiche ed evoluzione tettonica del settore esterno dell' Appennino meridionale: Bolletino della Società Geologica Italiana, v. 125, p. 39-58.

Do Couto, D., Gorini, C., Jolivet, L., Lebret, N., Augier, R., Gumiaux, C., d'Acremont, E., Ammar, A., Jabour, H., and Auxietre, J.-L., 2016, Tectonic and stratigraphic evolution of the Western Alboran Sea Basin in the last 25Myrs: Tectonophysics, v. 677-678, p. 280-311.

Do Couto D., Popescu S.-M., Suc J.-P., Melinte-Dobrinescu M.C., Barhoun N., Gorini C., Jolivet L., Poort J., Jouannic G., and Auxietre J.-L., 2014. Lago Mare and the Messinian Salinity Crisis: Evidences from the Alboran Sea (S. Spain). Marine and Petroleum Geology, 52, 57-76.

El Euch-El Kundi, N., Ferry, S., Suc, J.P., Clauzon, G., Melinte-Dobrinescu, M.C., Gorini, C., Safra, A., Zargouni, F.,, 2009, Messinian deposits and erosion in northern Tunisia: inferences on Strait of Sicily during the Messinian Salinity Crisis: Terra Nova, v. 21, p. 41-48.

983 Elter, P., Giglia, G., Tongiorgi, M., and Trevisan, L., 1975, Tensional and compressional areas in the
984 recent (Tortonian to Present) evolution of the Northern Apennines: Bollettino di Geofisica Te-
985 orica ed Applicata, v. 17, p. 3-18.
986 Esu, D., 2007, Latest Messinian "Lago-Mare" Lymnocardiinae from Italy: Close relations with the Pontian
987 fauna from the Dacic Basin: geobios, v. 40, p. 291-302.
988 Esu, D., Taviani, M., 1989. Oligohaline mollusc fauna of the Colombacci Formation (upper Messinian)
989 from an exceptional fossil vertebrate site in the Romagna Apennines: Monticino Quarry
990 (Brisighella, N Italy). Bolletino della Societa` Paleontologica Italiana 28, 265–270.
991 Fantoni, R., and Franciosi, R., 2008, 8 geological sections crossing Po Plain and Adriatic foreland: Ri-
992 assunti dell'84°. Congresso Nazionale Sassari 15–17 settembre 2008. Rend online Societa Geo-
993 logica Italia, v. 3, p. 367-368.
994 Fantoni, R., and Franciosi, R., 2010, Tectono-sedimentary setting of the Po Plain and Adriatic foreland:
995 Rend. Fis. Acc. Lincei, p. 197-209.
996 Faranda, C., Gliozzi, E., Ligios, S., 2007. Late Miocene brackish Loxoconchidae (Crustacea, Ostracoda)
997 from Italy. Geobios 40, 303–324.
998 Fauquette, S., Bernet, M., Suc, J.-P., Grosjean, A.-S., Guillot, S., van der Beek, P., Jourdan, S., Popescu,
999 S.-M., Jime´nez-Moreno, G., Bertini, A., Pittet, B., Tricart, P., Dumont, T., Schwartz, S., Zheng,
1000 Z., Roche, E., Pavia, G., Gardien, V., 2015a. Quantifying the Eocene to Pleistocene topographic
1001 evolution of the southwestern Alps, France and Italy. Earth and Planetary Science Letters 412,
1002 220–234.
1003 Fauquette, S., Bertini, A., Manzi, V., Roveri, M., Argnani, A., Menichetti, E., 2015b. Reconstruction of
1004 the Northern and Central Apennines (Italy) palaeoaltitudes during the late Neogene from pollen
1005 data. Review of Palaeobotany and Palynology 218, 117–126.
1006 Festa, V., Teofilo, G., Tropeano, M., Sabato, L., and Spalluto, L., 2013, New insights on diapirism in the
1007 Adriatic Sea: the Tremiti salt structure (Apulia offshore, southeastern Italy): Terra Nova, v. 0, p.
1008 1-10.
1009 Fidalgo-Gonzàlez, L., 2001, La cinématique de l'Atlantique Nord: la question de la déformation intra-
1010 plaque: Thèse de doctorat de l'Université de Bretagne Occidentale, Brest.
1011 Finetti, I.R., 1982, Structure, stratigraphy and evolution of central Mediterranean: Bolletino Di Geofisica
1012 Teorica Ed Applicata, v. 24, p. 247-312.
1013 Flecker, R., Krijgsman, W., Capella, W., de Castro Martins, C., Dmitriev, E., Mayser, J.P., Marzocchu, A.,
1014 Modestu, S., Ochoa, D., Simon, D., Tulbure, M., van der Berg, B., ven der Schee, M., de Lange,
1015 G., Ellam, R., Govers, R., Gutjah, M., Hilgen, F., Kouwenhoven, T.J., Lofi, J., Meijer, P., Sierro,
1016 F.J., Bachiri, N., Barhoun, N., Alami, A.C., Chacon, B., Flores, J.A., Gregory, J., Howard, J., Lunt,
1017 D., Ochoa, M., Pancost, R., Vincent, S., and Yousfi, M.Z., 2015, Evolution of the Late Miocene
1018 Mediterranean–Atlantic gateways and their impact on regional and global environmental change:
1019 Earth-Science Reviews, v. 150, p. 365-392.
1020 Fontes, J.-C., Filly, A., Gaudant, J., 1987. Conditions de dépôt du Messinien évaporitique des environs
1021 d'Alba (Piémont) : arguments paléontologiques et isotopiques. Bolletino della Societa` Paleonto-
1022 logica Italiana 26, 199–210.
1023 Frasheri, A., Bushati, S., and Bare, V., 2009, Geophysical outlook on structure of the Albanids: Journal
1024 of the Balkan Geophysical Society, v. 12, p. 9-30.
1025 Frasheri, A., Nishani, P., and Bushati, S., 1996, Relationship between tectonic zones of the Albanids,
1026 based on results of geophysical studies: Peri Tethys Memoir 2: Structure and Prospects of Alpine
1027 Basins and Forelands.: Hist. Nat., v. 170, p. 485-511.
1028 Funiciello, R., Montone, P., Parotto, M., Salvini, F., and Tozzi, M., 1991, Geodynamical evolution of an
1029 intra-orogenic foreland: The Apulia case history (Italy). Bolletino della Società Geologica Italiana,
1030 v. 110, p. 419-425.
1031 Garcia, M., Maillard, A., Aslanian, D., Rabineau, M., Alonso, B., Gorini, C., and Estrada, F., 2011, The
1032 Catalan margin during the Messinian Salinity Crisis: Physiography, morphology and sedimentary
1033 record: Marine Geology, v. 284, p. 158-174.

1034 Garcia-Castellanos, D., Estrada, F., Jiménez-Munt, L., Gorini, C., Fernandez, M., Vergès, J., and De Vi-
1035 cente, R., 2009, Catastrophic flood of the Mediterranean after the Messinian salinity crisis: Na-
1036 ture, v. 462, p. 778-781.
1037 Garcia-Castellanos, D., Micallef, A., Estrada, F., Camerlenghi, A., Ercilla, G., Periañez, R., and Abril, J.M.,
1038 2020, The Zanclean megaflood of the Mediterranean–Searching for independent evidence: Earth
1039 Science Reviews, v. 201.
1040 Gargani, J., Rigollet, C., and Scarselli, S., 2010, Isostatic response and geomorphological evolution of the
1041 Nile valley during the Messinian salinity crisis: Bull Soc. Géol. France, v. 181, p. 19-26.
1042 Gattacceca, J., and Speranza, F., 2002, Paleomagnetism of Jurassic to Miocene sediments from the Apen-
1043 ninic carbonate platform (southern Apennines, Italy) : evidence for a 60° counterclockwise Mio-
1044 cene rotation: Earth and planet. Sci. Lett., v. 201, p. 19-34.
1045 Giaconia, F., Booth-Rea, G., Ranero, C.R., Gracia, E., Bartolome, R., Calahorrano, A., Lo Iacono, C.,
1046 Vendrell, M.G., Cameselle, A.L., Coasta, S., Gomez de la Peña, L., Martinez-Loriente, S., Perea,
1047 H., and Viñas, M., 2015, Compressional tectonic inversion of the Algero-Balearic basin: Latemost
1048 Miocene to present oblique convergence at the Palomares margin (Western Mediterranean): Tec-
1049 tonics, v. 34.
1050 Gillet, S., 1968. La faune messinienne des environs d'Ancona avec une notice ge´ ologique par E. Ceretti.
1051 Giornale di Geologia 36 (1–4), 69–100.
1052 Ghielmi, M., Minervini, M., Nini, C., Rogledi, S., Rossi, M., and Vignolo, A., 2010, Sedimentary and
1053 tectonic evolution in the eastern Po-Plain and northern Adriatic Sea area from Messinian to Mid-
1054 dle Pleistocene (Italy): Rend. Fis. Acc. Lincei, v. 21, p. 131-166.
1055 Ghielmi, M., Minervini, M., Nini, C., Rogledi, S., and Rossi, M., 2013, Late Miocene - Middle Pleistocene
1056 Sequences In The Po-Plain - Northern Adriatic Sea (Italy): The Stratigraphic Record Of Modifi-
1057 cation Phases Affecting A Complex Foreland Basin: Marine and Petroleum Geology, v. 42, p. 50-
1058 51.
1059 Gliozzi, E., Ceci, M.E., Grossi, F., and Ligios, S., 2007, Paratethyan Ostracod immigrants in Italy during
1060 the Late Miocene: geobios, v. 40, p. 325-337.
1061 Gorini, C., Montadert, L., and Rabineau, M., 2015, New imaging of the salinity crisis: Dual Messinian
1062 lowstand megasequences recorded in the deep basin of both the eastern and western Mediterra-
1063 nean: Marine and Petroleum Geology, p. 1-17.
1064 Govers, R., Meijer, P., and Krijgsman, W., 2009, Regional isostatic response to Messinian Salinity Crisis
1065 events: Tectonophysics, v. 463, p. 109-129.
1066 Grubic, A., and Marovic, M., 1991, Tectonic features and genesis of the Scutari-Pec transverse in the
1067 Morka Gora area, Yugoslavia: Géologie Méditerranéenne, v. 18, p. 163-170.
1068 Gutcher, M.A., Kopp, H., Krastel, S., Bohrmann, G., Garlan, T., Zaragosi, S., Klaucke, I., Wintersteller,
1069 P., Loubrieu, B., Le Faou, Y., San Pedro, L., Dominguez, S., Rovere, M., Mercier De Lepinay, B.,
1070 Ranero, C., and Sallares, V., 2017, Active tectonics of the Calabrian subduction revealed by new
1071 multi-beam bathymetric data and high-resolution seismic profiles in the Ionian Sea (Central Med-
1072 iterranean): Earth and Planeary Science Letters, v. 461, p. 61-72.
1073 Hairabian, A., Borgomano, J., Masse, J.-P., and Nardon, S., 2015, 3-D stratigraphic architecture, sedimen-
1074 tary processes and controlling factors of Cretaceous deep-water resedimented carbonates (Gar-
1075 gano Peninsula, SE Italy): Sedimentary Geology, v. 317, p. 116-136.
1076 Handy, M.R., M. Schmid, S., Bousquet, R., Kissling, E., and Bernoulli, D., 2010. Reconciling plate-
1077 tectonic reconstructions of Alpine Tethys with the geological-geophysical record of spreading and
1078 subduction in the Alps: Earth-Science Reviews, v. 102, p. 121-158.
1079 Henriquet, M., Dominguez, S., Barreca, G., Malavieille, J., and Monaco, C., 2020, Structural and tectono-
1080 stratigraphic review of the Sicilian orogen and new insights from analogue modeling: Earth-Sci-
1081 ence Reviews, v. 208.
1082 Hilgen, F., Kuiper, K., Krijsgman, W., Snel, E., and Laan, E.V.D., 2007, Astronomical tuning as the basis
1083 for high resolution chronostratigraphy : the intricate history of the messinian salinity crisis: Stra-
1084 tigraphy, v. 4, p. 231-238.

1085 Hsü, K., Montadert, L., Bernouilli, D., Bizon, G., Cita, M., Erickson, A., Fabricius, F., Garrison, R.E.,
1086 Kidd, R.B., Mélières, F., Müller, C., and Wright, R.C., 1978, Initial Reports of the Deep Sea
1087 Drilling Project, DSDP Volume XLII.
1088 Iaccarino, S.M., Bertini, A., Di Stefano, A., Ferraro, L., Gennari, R., Grossi, F., Lirer, F., Manzi, V., Meni-
1089 chetti, E., Ricci Lucchi, F., Taviani, M., sturiale, G., and Angeletti, L., 2008, The Trave section
1090 (Monte dei Corvi, Ancona, Central Italy): an integrated paleontological study of the Messinian
1091 deposits: Stratigraphy, v. 5, p. 281-306.
1092 Kilias, A., Tranos, M., Mountrakis, D., Shallo, M., Marto, A., and Turku, I., 2001, Geometry and kine-
1093 matics of deformation in the Albanian orogenic belt during the Tertiary.: Journal of
1094 Geodynamics, v. 31, p. 169-187.
1095 Korbar, T., 2009, Orogenic evolution of the External Dinarides in the NE Adriatic region: a model
1096 constrained by tectonostratigraphy of Upper Cretaceous to Paleogene carbonates: Earth Science
1097 Reviews, v. 96, p. 296-312.
1098 Krijgsman, W., Garcès, M., Langereis, C.G., Daams, R., van Dam, J., van der Meulen, A.J., Agusti, J., and
1099 CABrera, L., 1996, A new chronology for the middle to late Miocene continental record in Spain:
1100 Earth and planet. Sci. Lett., v. 142, p. 367-380.
1101 Krijgsman, W., Leewis, M.E., Garcès, M., Kouwenhoven, T.J., Kuiper, K.F., and Sierro, F.J., 2006, Tec-
1102 tonic control for evaporite formation in the Eastern Betics (Tortonian; Spain): Sedimentary geol-
1103 ogy, v. 188-189, p. 155-170.
1104 Leever, K.A., Matenco, L., Garcia-Castellanos, D., and Cloetingh, S., 2010, The evolution of the Danube
1105 gateway between Central and Eastern Paratethys (SE Europe): Insight from numerical modelling
1106 of the causes and effects of connectivity between basins and its expression in the sedimentary
1107 record: Tectonophysics, v. 502, p. 175-195.
1108 Leroux, E., Aslanian, D., Rabineau, M., Moulin, M., Granjeon, D., Gorini, C., and Droz, L., 2015a,
1109 Sedimentary markers in the Provençal Basin (western Mediterranean): a window into deep geo-
1110 dynamic processes: Terra Nova, v. 27, p. 122-129.
1111 Leroux, E., Rabineau, M., Aslanian, D., Gorini, C., Bache, F., Moulin, M., Pellen, R., Granjeon, D., and
1112 Rubino, J.-L., 2015b, Post-rift evolution of the Gulf of Lion margin tested by stratigraphic model-
1113 ling: Bulletin de la société géologique de france, v. 186, p. 291-308.
1114 Leroux, E., Rabineau M., Aslanian D., Gorini C., Molliex S., Bache F., Robin C., Droz L., Moulin M.,
1115 Poort J., Rubino J.-L., Suc J.-P., 2017. High resolution evolution of terrigenous sediment yields in
1116 the Provence Basin during the last 6 Ma: relation with climate and tectonics: Basin Research, v.
1117 29 (3), p.305-339
1118 Leroux, E., Aslanian, D., Rabineau, M., Pellen, R., and Moulin, M., 2018, The late Messinian event: a
1119 worldwide tectonic upheaval: Terra Nova, v. 30, p. 207-214.
1120 Lofi, J., 2018, Seismic Atlas of the Messinian Salinity Crisis markers in the Mediterranean Sea - Volume
1121 2: Commission for the Geological Map of the World. Société Géologique de France, v. 2, p. 1-
1122 72.
1123 Lofi, J., Sage, F., Deverchère, J., Loncke, L., Maillard, A., Gaullier, V., Thinon, I., Gillet, H., Guennoc,
1124 P., and Gorini, C., 2011, Refining our knowledge of the Messinian Salinity crisis records in the
1125 offshore domaine through multi-site seismic analysis: Bulletin de la société géologique de france,
1126 v. 182, p. 163-180.
1127 Lugli, S., Manzi, V., Roveri, M., and Schreiber, B.C., 2010, The Primary Lower Gypsum in the Mediter-
1128 ranean: a new facies interpretation for the first stage of theMessinian salinity crisis.: Palaeogeog-
1129 raphy, Palaeoclimatology, Palaeoecology, v. 297, p. 83-99.
1130 Lymer, G., Lofi, J., Gaullier, V., Maillard, A., Thinon, I., Sage, F., Chanier, F., and Vendeville, B.C., 2018,
1131 The Western Tyrrhenian Sea revisited: New evidence for a rifted basin during the Messinian Sa-
1132 linity Crisis: Marine Geology, v. 398, p. 1-21.
1133 Madof, A.S., Bertoni, C., and Lofi, J., 2019, Discovery of vast fluvial deposits provides evidence for draw-
1134 down during the late Miocene Messinian salinity crisis: Geology, v. 47, p. 171-174.
1135 Maillard, A., Gorini, C., Mauffret, A., Sage, F., Lofi, J., and Gaullier, V., 2006, Offshore evidence of
1136 polyphase erosion in the Valencia Basin (Northwestern Mediterranean): Scenario for the Mes-
1137 sinian Salinity Crisis.: Sedimentary Geology, v. 188-189, p. 69-91.

Manzi, V., Argnani, A., Corcagnani, A., Lugli, S., and Roveri, M., 2020, The Messinian salinity crisis in the Adriatic foredeep: Evolution of the largest evaporitic marginal basin of the Mediterranean: Marine and Petroleum Geology, v. 115.

Manzi, V., Gennari, R., Hilgen, F., Krijgsman, W., Lugli, S., Roveri, M., and Sierro, F.J., 2013, Age refinement of the Messinian salinity crisis onset in the Mediterranean: Terra Nova, v. 25, p. 315-322.

Manzi, V., Gennari, R., Lugli, S., Persico, D., Regheizzi, M., Roveri, M., Schreiber, B.C., Calvo, R., Gavrieli, I., and Gvirtzman, Z., 2018, The onset of the Messinian salinity crisis in the deep Eastern Mediterranean basin: Terra Nova, v. 38, p. 42-49.

Manzi, V., Roveri, M., Gennari, R., Bertini, A., Biffi, U., Giunta, S., Iaccarino, S.M., Lanci, L., Lugli, S., Negri, A., Riva, A., Rossi, M.E., and Taviani, M., 2007, The deep-water counterpart of the Messinian Lower Evaporites in the Apennine foredeep: The Fanantello section (Northern Apennines, Italy): Palaeogeography, Palaeoclimatology, Palaeoecology.

Masters, J.C., Génin, F., Zhang, Y., Pellen, R., HUck, T., Mazza, P.P.A., Rabineau, M., Doucouré, M., and Aslanian, D., 2020, Biogeographic mechanisms involved in the colonization of Madagascar by African vertebrates: Rifting, rafting and runways: Journal of Biogeography, p. 1-19.

Matano, F., 2007, The 'Evaporiti di Monte Castello' deposits of the Messinian Southern Apennines foreland basin (Irpinia–Daunia Mountains, Southern Italy): stratigraphic evolution and geological context: Schreiber, B. C., Lugli, S. & Babel, M. (eds) Evaporites Through Space and Time. Geological Society, London, Special Publications, v. 285, p. 191-218.

Matano, F., Barbieri, M., Di Nocera, S., and Torre, M., 2005, Stratigraphy and strontium geochemistry of Messinian evaporite-bearing successions of the southern Apennines foredeep, Italy: implications for the Mediterranean "salinity crisis" and regional palaeogeography: Palaeogeography, Palaeoclimatology, Palaeoecology, v. 217, p. 87-114.

Matano, F., Critelli, S., Barone, M., Muto, F., and Di Nocera, S., 2014, Stratigraphic and provenance evolution of the Southern Apennines foreland basin system during the Middle Miocene to Pliocene (Irpinia-Sannio successions, Italy): Marine and Petroleum Geology, v. 57, p. 652-670.

Matias, L., Olivet, J.-L., Aslanian, D., and Fidalgo, L., 2005, PLACA: a white box for plate reconstruction and best-fit pole determination: Computer & Geosciences, v. 31, p. 437-452.

Mazzoli, S., D'Errico, M., Aldega, L., Corrado, S., Invernizzi, C., Shiner, P., and Zattin, M., 2008, Tectonic burial and "young" (<10 Ma) exhumation in the southern Apennines fold-and-thrust belt (Italy): Geological Society of America, v. 36, p. 243-246.

Mele, G., 2001, The Adriatic lithosphere is a promontory of the African plate: Evidence of a continuous mantle lid in the Ionian Sea from efficient Sn propagation: Geophysical Research Letters, v. 28, p. 431-434.

Micallef, A., Camerlenghi, A., Garcia-Castellanos, D., Otero, D.C., Gutscher, M.-A., Barreca, G., Spatola, D., Facchin, L., Geletti, R., Krastel, S., Gross, F., and Urlaub, M., 2018, Evidence of the Zanclean megaflood in the eastern Mediterranean basin: Nature Scientific Reports, v. 8.

Milli, S., Moscatelli, M., Stanzione, O., Falcini, F., and Bigi, S., 2006, The Messinian Laga Formation, facies, geometries, stratigraphic architecture and structural style of a confined turbidite basin (Central Apennines, Italy). Excursion Guidebook, Field Trip 17-21 Settembre 2006.

Milli, S., Moscatelli, M., Stanzione, O., and Falcini, F., 2007, Sedimentology and physical stratigraphy of the Messinian turbidite deposits of the Laga Basin (central Apennines, Italy): Bolletino della Società Paleontologica Italiana, v. 126, p. 255-281.

Morelli, D., 2002, Evoluzione tettonico-stratigrafica del Margine Adriatico compreso tra il Promontorio garganico e Brindisi: Memory di Societa Geologica Italia, v. 57, p. 343-353.

Moscardelli, L., and Wood, L., 2007, New classification system for mass transport complexes in offshore Trinidad: Basin Research, v. 20, p. 73-98.

Moulin, M., Klingelhoefer, F., Afilhado, A., Aslanian, D., Schnurle, P., Nouzé, H., Rabineau, M., Beslier, M.-O., and Feld, A., 2015, Deep crustal structure across a young passive margin from wide-angle and reflection seismic data (The SARDINIA Experiment) – I. Gulf of Lion's margin: Bulletin de la société géologique de france, v. 186, p. 309-330.

Ori, G.G., Serafini, G., Visentin, C., Ricci Lucchi, F., Casnedi, R., Colalongo, M.L., and Mosna, S., 1991, The Pliocene-Pleistocene Adriatic Foredeep (Marche and Abruzzo, Italy): an integrated approach to surface and subsurface geology.: In: Agip-EAPG (Ed.), 3rd EAPG Conference. Adriatic Foredeep Field Trip, Florence May 26-30, p. 85.

Palcu, D.V., Golovina, L.A., Vernyhorova, Y.V., Popov, S.V., and Krijgsman, W., 2017, Middle Miocene paleoenvironmental crises in Central Eurasia caused by changes in marine gateway configuration: Global and Planetary Change, v. 158, p. 57-71.

Panza, G.F., Pontevivo, A., Chimera, G., Raykova, R., and Aoudia, A., 2003, The lithosphere–astenosphere: Italy and surroundings: Episodes, v. 26, p. 168-173.

Pashko, P., and Aliaj, S., 2020, Stratigraphy and tectonic evolution of late Miocene-Quaternary basins in Eastern Albania: a review: Bulletin Geological Society of Greece, v. 56, p. 317-351.

Patacca, E., Scandone, P., and Mazza, P., 2008, Oligocene migration path for Apulia macromammals: the Central-Adriatic bridge: Bollettino della Societa Geologica Italiana, v. 127, p. 337-355.

Pedley, M., Grasso, M., Maniscalco, R., and Esu, D., 2007, The Monte Carrubba Formation (Messinian, Sicily) and its correlatives: New light on basin-wide processes controlling sediment and biota distributions during the Palaeomediterranean - Mediterranean transition: Palaeogeography Palaeoclimatology Palaeoecology, v. 253, p. 363-384.

Pelleau, P., Aslanian, D., Matias, L., Moulin, M., Augustin, J.-M., Quemener G. & Poncelet C., 2015. Placa4D freeware: a new interactive tool for palinspastic reconstruction in 3D, AAPG congres, Lisbonne.

Pellen, R., 2016, Géodynamique et impact de la crise d'érosion et de salinité Messinienne sur les transferts sédimentaires (bassin de Valence, bassin Adriatique): Thèse de doctorat - Sciences de la Terre. Université Bretagne Occidentale, p. 550 p.

Pellen, R., Aslanian, D., Rabineau, M., Suc, J.P., Gorini, C., Leroux, E., Blanpied, C., Silenziario, C., Popescu, S.-M., and Rubino, J.L., 2019, The Messinian Ebro River incision: Global and Planetary Change, v. 181.

Pellen, R., Aslanian, D., Rabineau, M., 2021. A comprehensive compilation of the seismic stratigraphy markers along the Adriatic Sea. SEANOE. https://doi.org/10.17882/84576

Pellen, R., Popescu, S.-M., Suc, J.P., Melinte-Dobrinescu, M.C., Rubino, J.-L., Rabineau, M., Marabini, S., Loget, N., Casero, P., Cavazza, W., Head, M.J., and Aslanian, D., 2017, The Apennine foredeep (Italy) during the latest Messinian: Lago Mare reflects competing brackish and marine conditions based on calcareous nannofossils and dinoflagellate cysts: Geobios, v. 50, p. 237–257.

Pescatore, T.S., Di Nocera, S., Matano, F., Pinto, F., Boiano, U., Civile, D., Martino, C., and Quarantiello, R., 2008, Prime considerazioni sulla geologia del settore centrale dei monti del Sannio: Memorie Descr. Carta Geol. It., v. 77, p. 77-94.

Petrullo, A.V., Agosta, F., Prosser, G., and Rizzo, E., 2017, Cenozoic tectonic evolution of the northern Apulian carbonate Platform (southern Italy): Italian Journal of Geosciences, v. 136, p. 1-16.

Popescu S.-M., Dalibard M., Suc J.-P., Barhoun N., Melinte-Dobrinescu M.C., Bassetti M.A., Deaconu F., Head M.J., Gorini C., Do Couto D., Rubino J.-L., Auxietre J.-L., Floodpage J., 2015. Lago Mare episodes around the Messinian–Zanclean boundary in the deep southwestern Mediterranean. Marine and Petroleum Geology, 66, 1, 55-70.

Popescu, S.M., Melinte, M.-C., Suc, J.-P., Clauzon, G., Quillévéré, F., and Süto-Szentai, M., 2007, Earliest Zanclean age for the Colombacci and uppermost Di Tetto formations of the ''latest Messinian'' northern Apennines: New palaeoenvironmental data from the Maccarone section (Marche Province, Italy): Geobios, v. 40, p. 359-373.

Popescu, S.M., Melinte, M-C., Suc, J.-P., Clauzon, G., Quillévéré, F., Süto-Szentai, M.,, 2008, Comment on Marine reflooding of the Mediterranean after the Messinian Salinity Crisis predates the Zanclean GSSP. Reply to the ''Comment on 'Earliest Zanclean age for the Colombacci and uppermost Di Tetto formations of the ''latest Messinian'' northern Apennines: New palaeoenvironmental data from the Maccarone section (Marche Province, Italy)' by Popescu *et al.* (2007) Geobios 40 (359–373)'' authored by Roveri *et al.*: Geobios, v. 41, p. 657-660.

Popescu, S.-M., Cavazza, W., Suc, J.-P., Melinte-Dobrinescu, M.C., Barhoun, N., and Gorini, C., 2021, Pre-Zanclean end of the Messinian Salinity Crisis: new evidence from central Mediterranean reference sections: Journal of the Geological Society, v. 178, p. 1-16.

Rabineau, M., Leroux, E., Bache, F., Aslanian, D., Gorini, C., Moulin, M., Molliex, S., Droz, L., Reis, T.D., Rubino, J.-L., and Olivet, J.-L., 2014, Quantifying subsidence and isostatic readjustment using sedimentary paleomarkers, example from the Gulf of Lion: Earth and planetary Science Letters, v. 388, p. 1-14.

Ricci Lucchi, F., 1986, The Oligocene to Recent foreland basins of the northern Apennines: Spec. Publs. int. Ass. Sediment, v. 8, p. 105-139.

Riguzzi, F., and Doglioni, C., 2020, Gravity and crustal dynamics in Italy: Rendiconti Lincei. Scienze Fisiche e Naturali volume, v. 31, p. 49-58.

Ritzwoller, M.H., Yang, Y., Richmond, R.M., Pasyanos, M.E., Villasenor, A., Levin, V., Hofstetter, R., Pinsky, V.I., Kraeva, N.V., and Lerner-Lam, A., 2007, Short Period Surface Wave Dispersion Across the Mediterranean Region: Improvements Using Regional Seismic Networks: 29th Monitoring Research Review: Ground-Based Nuclear Explosion Monitoring Technologies. Conference paper.

Rossi, M., Minervini, M., Ghielmi, M., and Rogledi, S., 2015, Messinian and Pliocene erosional surfaces in the Po Plain-Adriatic Basin: Insights from allostratigraphy and sequence stratigraphy in assessing play concepts related to accommodation and gateway turnarounds in tectonically active margins: Marine and Petroleum Geology, v. 66, p. 192-216.

Roure, F., Casero, P., and Addoum, B., 2012, Alpine inversion of the North African margin and delamination of its continental lithosphere: Tectonics, v. 31, p. TC3006.

Roveri, M., Bassetti, M.A., and Ricci Lucchi, F., 2001, The Mediterranean Messinian Salinity Crisis: an Apennine foredeep perspective. : Sedimentary Geology, v. 140.

Roveri, M., Boscolo Gallo, A., Rossi, M., Gennari, R., Iaccarino, S.M., Lugli, S., Manzi, V., Negri, A., Rizzini, F., and Taviani, M., 2005, The Adriatic foreland record of Messinian events (Central Adriatic Sea, Italy): GeoActa, v. 4.

Roveri, M., Flecker, R., Krijgsman, W., Lofi, J., Lugli, S., Manzi, V., Sierro, F.J., bertini, A., Camerlenghi, A., De Lange, G., Govers, R., Hilgen, F.J., Hübscher, C., Meijer, P.T., and Stoica, M., 2014, The Messinian Salinity Crisis: Past and future of a great challenge for marine sciences: Marine Geology, v. 352, p. 25-58.

Roveri, M., Gennari, R., Lugli, S., Manzi, V., Minelli, N., Reghezzi, M., Riva, A., Rossi, M.E., and Schreiber, B.C., 2016, The Messinian salinity crisis: open problems and possible implications for Mediterranean petroleum systems: Petroleum Geoscience.

Roveri, M., Landuzzi, A., Bassetti, M.A., Lugli, S., Manzi, V., Ricci Lucchi, F., and Vai, G.B., 2004, The record of Messinian events in the northern Apennines foredeep basins: Pre-congress guide of the 32nd International Geological congress v. 2.

Roveri, M., Lugli, S., Manzi, V., and Schreiber, B.C., 2008a, The Messinian Sicilian stratigraphy revisited: new insights for the Messinian salinity crisis: Terra Nova, v. 20, p. 483-488.

Roveri, M., and Manzi, V., 2006, The Messinian salinity crisis: Looking for a new paradigm?: Palaeogeography, Palaeoclimatology, Palaeoecology, v. 238, p. 386-398.

Roveri, M., Manzi V., Bassetti M.A., Merini M., and Ricci Lucchi F., 1998, Stratigraphy of the Messinian post-evaporitic stage in eastern-Romagna (northern Apennines, Italy): Giornale di Geologia, v. 60, p. 119-142.

Roveri, M., Manzi, V., Gennari, R., Iaccarino, S., and Lugli, S., 2008b, Recent advancements in the Messinian stratigraphy of Italy and their Mediterranean-scale implications. : Bolletino della Società Paleontologica Italiana, v. 47, p. 71–85.

Sage, F., Von Gronefeld, G., Déverchère, J., Gaullier, V., Maillard, A., and Gorini, C., 2005, Seismic evidence for Messinian detrital deposits at the western Sardinia margin, northwestern Mediterranean: Marine and Petroleum Geology, v. 22, p. 757-773.

Schmid, S.M., Bernouilli, D., Fügenschuh, B., Matenco, L., Schefer, S., Schuster, R., Tischler, M., and Ustaszewski, K., 2008, The Alpine-Carpathian-Dinaridic orogenic system: correlation and evolution of tectonic units: Swiss Journal of Geosciences, v. 101, p. 139-183.

1294 Scisciani, C., and Calamita, F., 2009, Active intraplate deformation within Adria: Examples from the
1295 Adriatic region: Tectonophysics, v. 476, p. 57-72.
1296 Scrocca, D., 2006, Thrust front segmentation induced by differential slab retreat in the Apennines (Italy):
1297 Terra Nova, v. 18, p. 154-161.
1298 Selli, R., 1960, Il Messiniano Mayer-Eymar 1867. Proposta di un neostratotipo: Giornale di Geologia, v.
1299 28, p. 1-33.
1300 Selli, R., 1973, Il Mediterraneo nel Miocene superiore: un mare sovrasalato: Scienze, v. 56, p. 20-21.
1301 Shiner, P., Beccacini, A., and Mazzoli, S., 2004, Thin-skinned versus thick-skinned structural models for
1302 Apulian Carbonate Reservoirs: constraints from the Val D'Agri Fields: Marine and Petroleum
1303 Geology, v. 21, p. 805-827.
1304 Silo, V., Muska, K., and Silo, E., 2013, Hydrocarbon evaluation aspects in Molasse reservoirs, Vlorë-El-
1305 basan region, Albania: Italian Journal of Geosciences.
1306 Sioni, S., 1996, Mer Ionienne et Apulie depuis l'ouverture de l'Océan Alpin. Thèse de Doctorat, Univer-
1307 sité de Bretagne Occidentale.
1308 Sprovieri, M., Ribera d'Alcalà, M., Manta, D.S., Bellanca, A., Neri, R., Lirer, F., Taberner, C., Pueyo, J.J.,
1309 and Sammartino, S., 2008, Ba/Ca evolution in water masses of the Mediterranean late Neogene.
1310 Paleoceanography v. 23.
1311 Stampfli, G.M., and Hochard, C., 2009, Plate tectonics of the Alpine realm: Geological Society, London,
1312 Special Publication, v. 327, p. 89-111.
1313 Sternai, P., Caricchi, L., Garcia-Castellanos, D., Jolivet, L., Sheldrake, T.E., and Castelltort, S., 2017,
1314 Magmatic pulse driven by sea-level changes associated with the Messinian salinity crisis: Nature
1315 Geoscience, p. 1-5.
1316 Straume, E.T., Gaina, C., Medvedev, S., and Nisancioglu, K.H., 2020, Global Cenozoic Paleobathymetry
1317 with a focus on the Northern Hemisphere Oceanic Gateways: Gondwana Research, v. 86, p. 126-
1318 143.
1319 Sturani, C., 1973. A fossil eel (Anguilla sp.) from the Messinian of Alba (Tertiary Piedmontese Basin).
1320 Palaeoenvironmental and palaeogeographic implications. In: Drogger, C.W., Broekman, J.A.,
1321 Hageman, J., Hantelman, J.J., Marks, P., Meulenkamp, J.E., Schmidt, R.R. (Eds.), Messinian
1322 events in the Mediterranean. Koninklijke Nederlandse Akademie Van Wetenschappen. North-
1323 Holland Pub-lishing Company, Amsterdam, London, pp. 243–255.
1324 Suc, J.-P., Do Couto, D., Melinte-Dobrinescu, M.C., Macalet ¸ , R., Quillévéré, F., Clauzon, G., Csato, I.,
1325 Rubino, J.-L., and Popescu, S.-M., 2011, The Messinian Salinity Crisis in the Dacic Basin (SW
1326 Romania) and early Zanclean Mediterranean-Paratethys high sea-level connection. : Palaeogeogra-
1327 phy, Palaeoclimatology, Palaeoecology, v. 310, p. 256-272.
1328 Suc, J.-P., Popescu, S.-M., Do Couto, D., Clauzon, G., Rubino, J.-L., Melinte-Dobrinescu, M.C., Quil-
1329 lévéré, F., Brun, J.-P., Dumurdzanov, N., Zagorchev, I., Lesic, V., Tomic, D., Sokoutis, D., Meyer,
1330 B., Macalet, R., and Rifelj, H., 2015, Marine gateway vs. fluvial stream within the Balkans from 6
1331 to 5 Ma: Marine and Petroleum Geology, v. 66, p. 231-245.
1332 Tondi, E., Piccardi, L., Cacon, S., Kontny, B., and Cello, G., 2005, Structural and time constraints for
1333 dextral shear along the seismogenic Mattinata fault (Gargano, southern Italy): Journal of Geody-
1334 namics, v. 40, p. 134-152.
1335 van Hinsbergen, D.J.J., Langereis, C.G., and Meulenkamp, J.E., 2004, Revision of the timing, magnitude
1336 and distribution of Neogene rotations in the western Aegean region: Tectonophysics, v. 396, p.
1337 1-34.
1338 van Hinsbergen, D.J.J., and Schmid, S.M., 2012, Map view restoration of Aegean-West Anatolian accre-
1339 tion and extension since the Eocene: Tectonics, v. 31.
1340 van Hinsbergen, D.J.J., Torsvik, T.H., Schmid, S.M., Matenco, L.C., Maffione, M., Vissers, R.L.M., Gürer,
1341 D., and Spakman, W., 2020, Orogenic architecture of the Mediterranean region and kinematic
1342 reconstruction of its tectonic evolution since the Triassic: Gondwana Research, v. 81, p. 79-229.
1343 van Hinsbergen, D.J.J., and Schmid, S.M., 2012, Map view restoration of Aegean-West Anatolian
1344 accretion and extension since the Eocene: Tectonics, v. 31.
1345 Vezzani, F., Festa, A., and Ghisetti, F.C., 2010, Geology and Tectonic Evolution of the Central-Southern
1346 Apennines, Italy: The Geological Society of America, Special Paper, v. 469, p. 58 pp.

Violanti, D., Gallo, L.M., and Rizzi, A., 2007, Foraminiferal assemblages of the Bric della Muda laminites (Nizza Monferrato, Piedmont): proxies of cyclic paleoenvironmental changes in the Lower Messinian of Northwestern Italy.: Geobios, v. 40, p. 281-290.

Violanti, D., Dela Pierre, F., Trenkwalder, S., Lozar, F., Clari, P., Irace, A., and D'Atri, A., 2011, Biostratigraphic and palaeoenvironmental analyses of the Messinian/Zanclean boundary and Zanclean succession in the Moncucco quarry (Piedmont, northwestern Italy): Bulletin de la Société Géologique de France, v. 182, p. 149-162.

Vitale, S., and Ciarcia, S., 2013, Tectono-stratigraphic and kinematic evolution of the southern Apennines/Calabria–Peloritani Terrane system (Italy): Tectonophysics, v. 583, p. 164-182.

Wrigley, R., Hodgson, N. and Esestime, P. 2015, Petroleum geology and hydrocarbon potential of the Adriatic Basin, offshore Croatia: Journal of Petroleum Geology, Vo. 38 (3), pp. 301-316.

Zappaterra, E., 1994, Source-Rock distribution model of the Periadriatic region The American Association of Petroleum Geologists Bulletin, v. 78, p. 333-354.

Zarcone, G., Petti, F.M., Cillari, A., Di Stefano, P., Guzetta, D., and Nicosia, U., 2010, A possible bridge between Adria and Africa: New palaeobiogeographic and stratigraphic constraints on the Mesozoic palaeogeography of the Central Mediterranean area: Earth-Science Reviews, v. 103, p. 154-162.

Figure

Figure 1: Physiographic map of the Mediterranean highlighting the main oceanic gateways (in light red) during the Last Glacial Maximum and during the Neogene. The color scale is adapted to the LGM sea level and highlight the main present-day gateways. These gateways control the water, sediment, and biotope exchange between sub-basins and oceans.

Figure 2: Illustration of the general palaeoenvironmental and structural framework compiled from Vezzani *et al.*, (2010); Bigi *et al.*, (1990); van Hinsbergen *et al.*, (2020). The structural zones are associated with the deformation fronts of the Apennines, Dinarids and Albano-Hellenid (synthetized from Zappaterra, 1994; Vezzani *et al.*, 2010; van Hinsbergen *et al.*, 2020; this study). Sestri-Voltaggio lineament (S.V.); the Anzio-Ancona lineament (A.A.); Maiella-Roccamonfina lineament (M.R.); M.A.R. – Mid-Adriatic Ridge; T.R. – Tremiti Ridge; M.F.S. –Mattinata Fault System; CAB – Central Adriatic Basin; SAB – South Adriatic Basin.

Figure 3: Synthesis of the evolution of the Cenozoic deposit environments specific to each palaeogeographic domain developed during the Mesozoic (synthesized from Vezzani *et al.*, 2010). The involvement of palaeogeographic domain inside the fold-and-thrust belt and the associated wedge-top formation are represented in orange. Major tectonic phase reported by Vezzani *et al.* (2010) are highlighted in light red and numbered from 1 to 6.

Figure 4:
Previously published MSC formations along the Central Mediterranean area.
Liguri-Provence Basin (Sage *et al.*, 2005; Lofi *et al.*, 2011; Bache *et al.*, 2015). Tyrrhenian Sea (Lymer *et al.*, 2018). **Sicily and Calabria** (Butler *et al.*, 1995, 2019 ; Pedley *et al.*, 2007; El Euch-El Kundi *et al.*, 2009; Roveri *et al.*, 2008a; Henriquet *et al.*, 2020 ; Cavazza and DeCelles, 1998). **Northern and Central Apennine Chain** (Roveri *et al.*, 2005, 2008b; Ghielmi *et al.*, 2013; Rossi *et al.*, 2015; Pellen *et al.*, 2017; Manzi *et al.*, 2013, 2020; Iaccarino *et al.*, 2008; Milli *et al.*, 2006, 2007; Artoni, 2003; Bigi *et al.*, 2009). **South Apennine Chain** (Vezzani *et al.*, 2010; Manzi *et al.*, 2020). **South Adriatic Basin** (Frasheri *et al.*, 2009; Silo *et al.*, 2013; Argnani *et al.*, 2009). **Ionian Basin** (Micallef *et al.*, 2018 ; Garcia-Castellanos *et al.*, 2020 ; Gutcher *et al.*, 2017).

Table 01: Correlation table of the different deposit units identified along the Apennine foredeep by [Milli *et al.*, 2007] compared to the nomenclature of Roveri *et al.* [2004, 2005].
Legend: pre-ev: pre-evaporitic unit; post-ev: post-evaporitic unit. U1, U2, U3 and I1, I2, I3 are non-conforming surfaces. The dashed line indicates the position of the cinerite level.

Figure 5: Map showing our new interpretation of the sedimentary facies and stratigraphic units observed along the Adriatic Sea and associated with the Messinian event. The mapping of geological formations on land refers to that used in the figure 4. The Messinian-Pliocene basal (yellow to bluish) and Tortonian (pinkish) deposits are highlighted.

Table 02: Stratigraphic chart correlation

Figure 6a: Stratigraphic correlation between 6 boreholes selected on both sides of the promontory of Gargano. This synthesis highlights a different sedimentary filling dynamics in the Tertiary between the CAB (Central Adriatic Basin) and SAB (South Adriatic Basin).

Figure 6b: Illustration of three stratigraphic sections based on industrial boreholes along the CAB and SAB. Significant Oligocene-Tortonian depocenter is observed within the SAB, while strong depocenter is observed during the Pliocene-Quaternary within the CAB.

Figure 7: SW-NE oriented line-drawings along the CAB.

Figure 8: SW-NE oriented line-drawings along the SAB.

Figure 9: Detailed seismic sections (location Figure 8) highlighting the initiation (left) and lateral evolution (right) of the Mass Transport Deposit which mainly compose the M3 seismic unit. The lateral transition from chaotic to continuous seismic reflections allowed to identify the western limit of the MTD observed on Figure 5.

Table 3: Retro-translation and back-rotation values of Adria, Africa, and Calabria-Peloritain blocks with respect to stable Europe (and Corsica-Sardinia blocks). Sources: Sioni (1996); Fidalgo-Gonzàlez (2001), this study.

Figure 10:
A (Top): Palinspastic reconstruction of the Central Mediterranean area at 7.2 Ma.
B (Bottom): Palaeoenvironmental reconstruction of the Central Mediterranean area at 7.2 Ma.

Figure 11:
A (Top): Palinspastic reconstruction of the Central Mediterranean area at 5.9 Ma.
B (Bottom): Palaeoenvironmental reconstruction of the Central Mediterranean area at 5.9 Ma.

Figure 12:
A (Top): Palinspastic reconstruction of the Central Mediterranean area at 5.6 Ma.
B (Bottom): Palaeoenvironmental reconstruction of the Central Mediterranean area at 5.6 Ma.

Figure 13:
A (Top): Palinspastic reconstruction of the Central Mediterranean area at 5.5 Ma.
B (Bottom): Palaeoenvironmental reconstruction of the Central Mediterranean area at 5.5 Ma.

Figure 14:
A (Top): Palinspastic reconstruction of the Central Mediterranean area at 5.36 Ma.
B (Bottom): Palaeoenvironmental reconstruction of the Central Mediterranean area at 5.36 Ma.

Figure 15:
A (Top): Palinspastic reconstruction of the Central Mediterranean area at 5.3 Ma.
B (Bottom): Palaeoenvironmental reconstruction of the Central Mediterranean area at 5.3 Ma.

Figure 16:
Monte Ferrara section belonging to the evaporitic Formation of the Castello Mounts, located SE of the Gargano Peninsula (Geographic location Figure 5). The base of the MSC Monte Ferrara succession lies conformably on the Serravallian-Tortonian Serra Palazzo Fm., where primary gypsum facies (massive, banded and branching selenite) are defined.

A major unconformity erodes the Primary Lower Gypsum, then overlapped by pluri-decametric PLG blocks and rich gypso-aneritic beds composing the Resedimented Lower Gypsum. Desiccation cracks and brecciated deposits at the level of the angular unconformity suggest a possible subaerial exposure of the whole Castello Evaporitic Fm. along the south Apennine Chain.

Supplementary material 1: Non-interpreted SW-NE oriented seismic profiles along the CAB. Confidential agreement with Spectrum did not allow us to publish the seismic profiles of the CRO132D campaign.

Supplementary material 2: Non-interpreted SW-NE oriented seismic profiles along the SAB. Confidential agreement with Spectrum did not allow us to publish the seismic profiles of the CRO132D campaign.

Figure 01

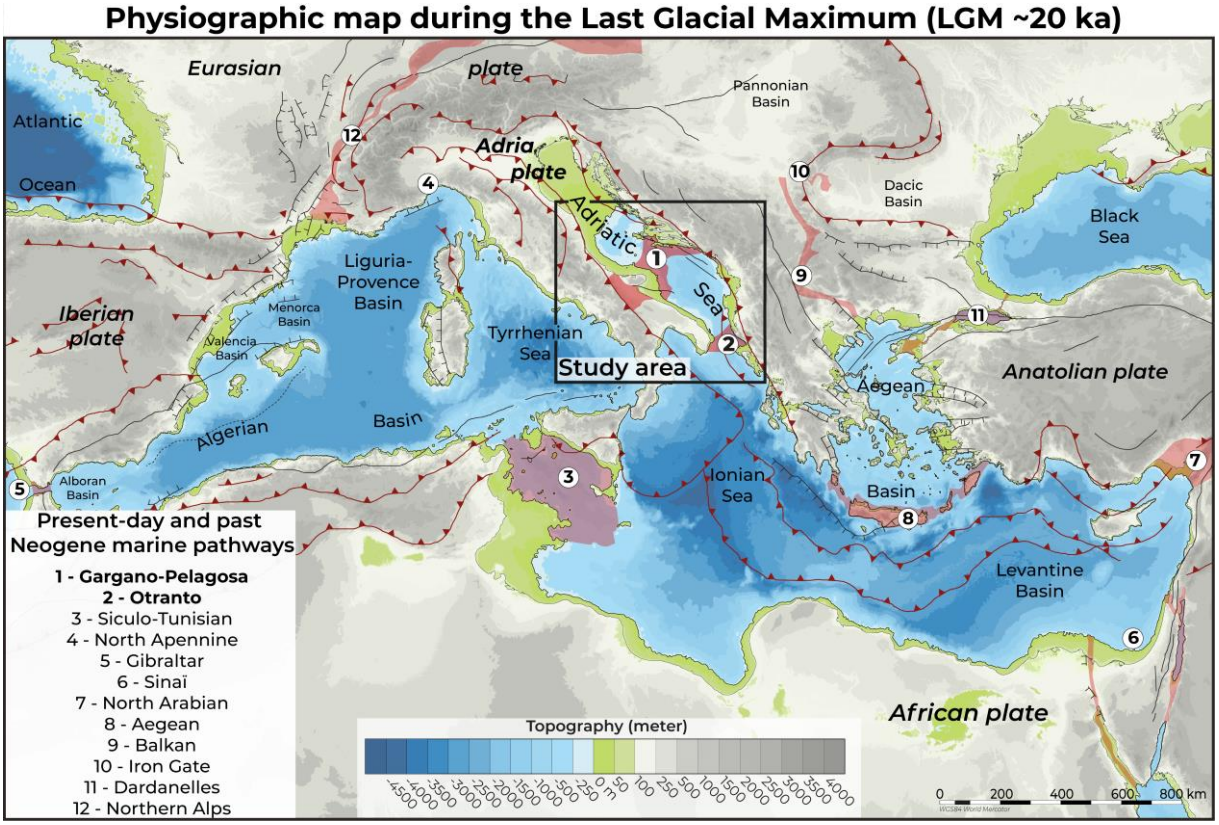
Physiographic map during the Last Glacial Maximum (LGM ~20 ka)
Eurasian plate
Atlantic Ocean
Iberian plate
Adria plate
Pannonian Basin
Dacic Basin
Black Sea
Liguria-Provence Basin
Menorca Basin
Valencia Basin
Algerian Basin
Alboran Basin
Tyrrhenian Sea
Adriatic Sea
Study area
Aegean
Anatolian plate
Ionian Sea
Basin
Levantine Basin
African plate
Present-day and past Neogene marine pathways
1 - Gargano-Pelagosa
2 - Otranto
3 - Siculo-Tunisian
4 - North Apennine
5 - Gibraltar
6 - Sinaï
7 - North Arabian
8 - Aegean
9 - Balkan
10 - Iron Gate
11 - Dardanelles
12 - Northern Alps
Topography (meter)
-4500 -4000 -3500 -3000 -2500 -2000 -1500 -1000 -500 -250 0 m 50 100 250 500 1000 1500 2000 2500 3000 3500 4000
0 200 400 600 800 km

1382

Figure 02

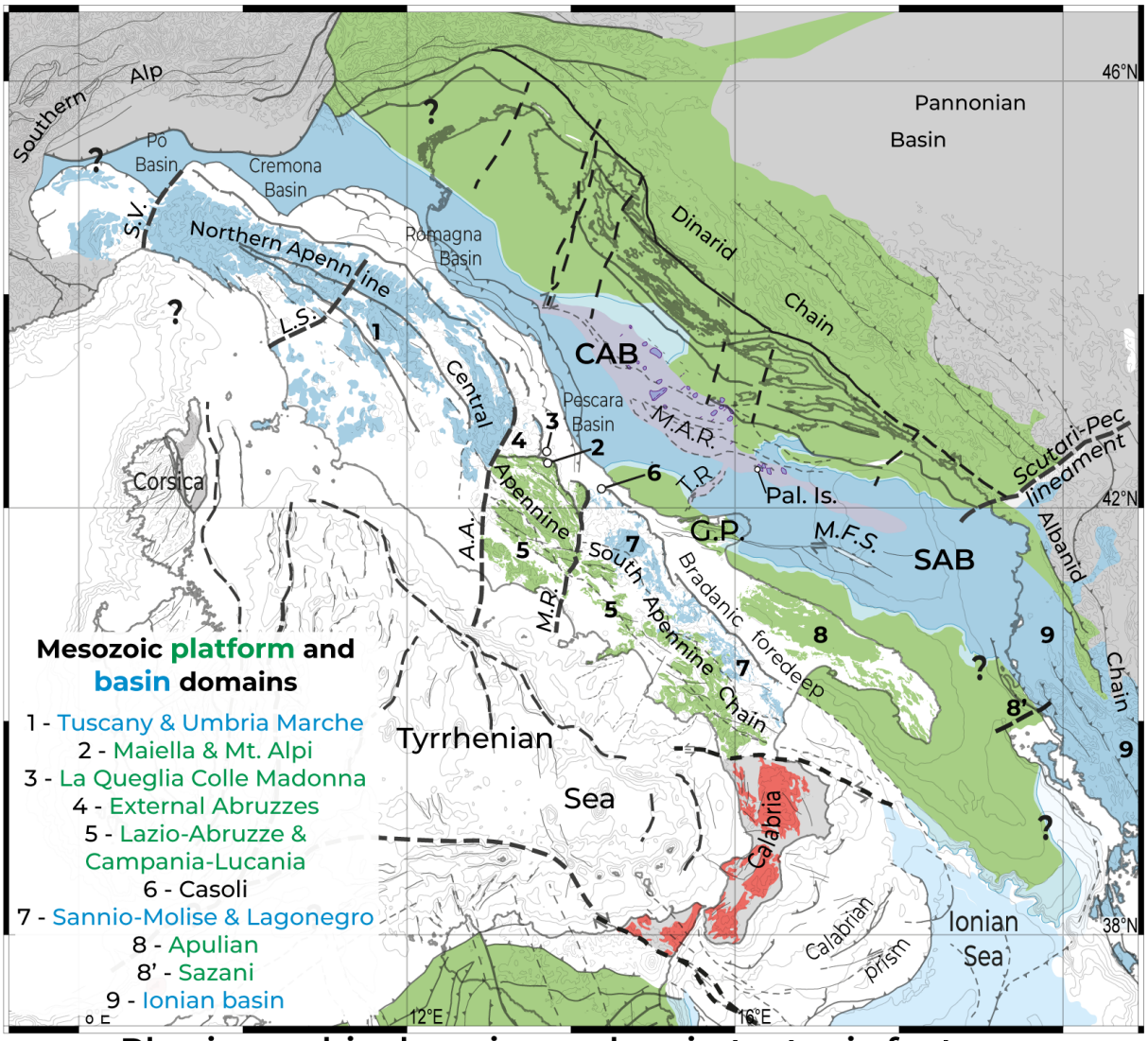

1383

1384

Figure 03

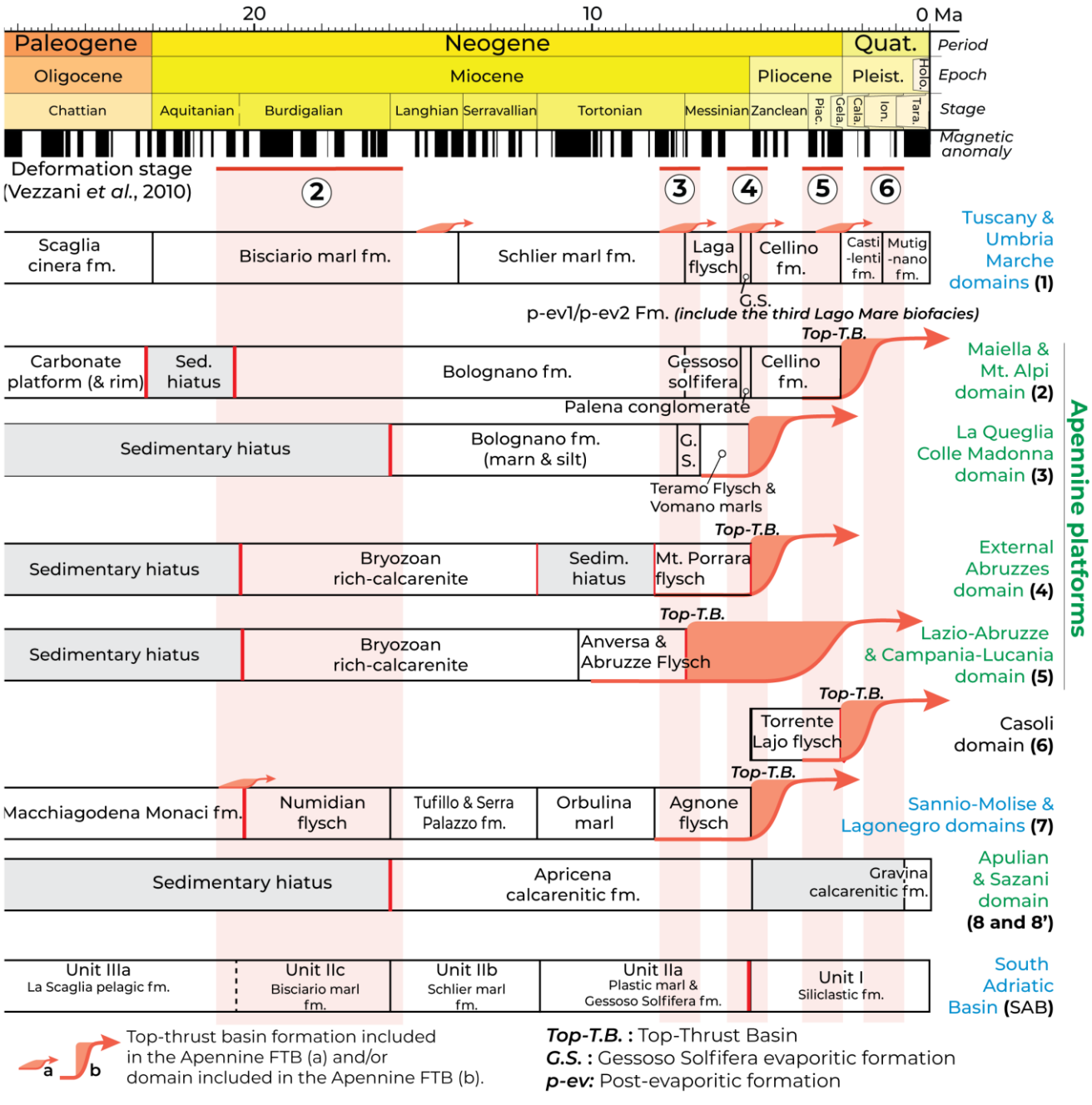

1385

1386

Figure 04

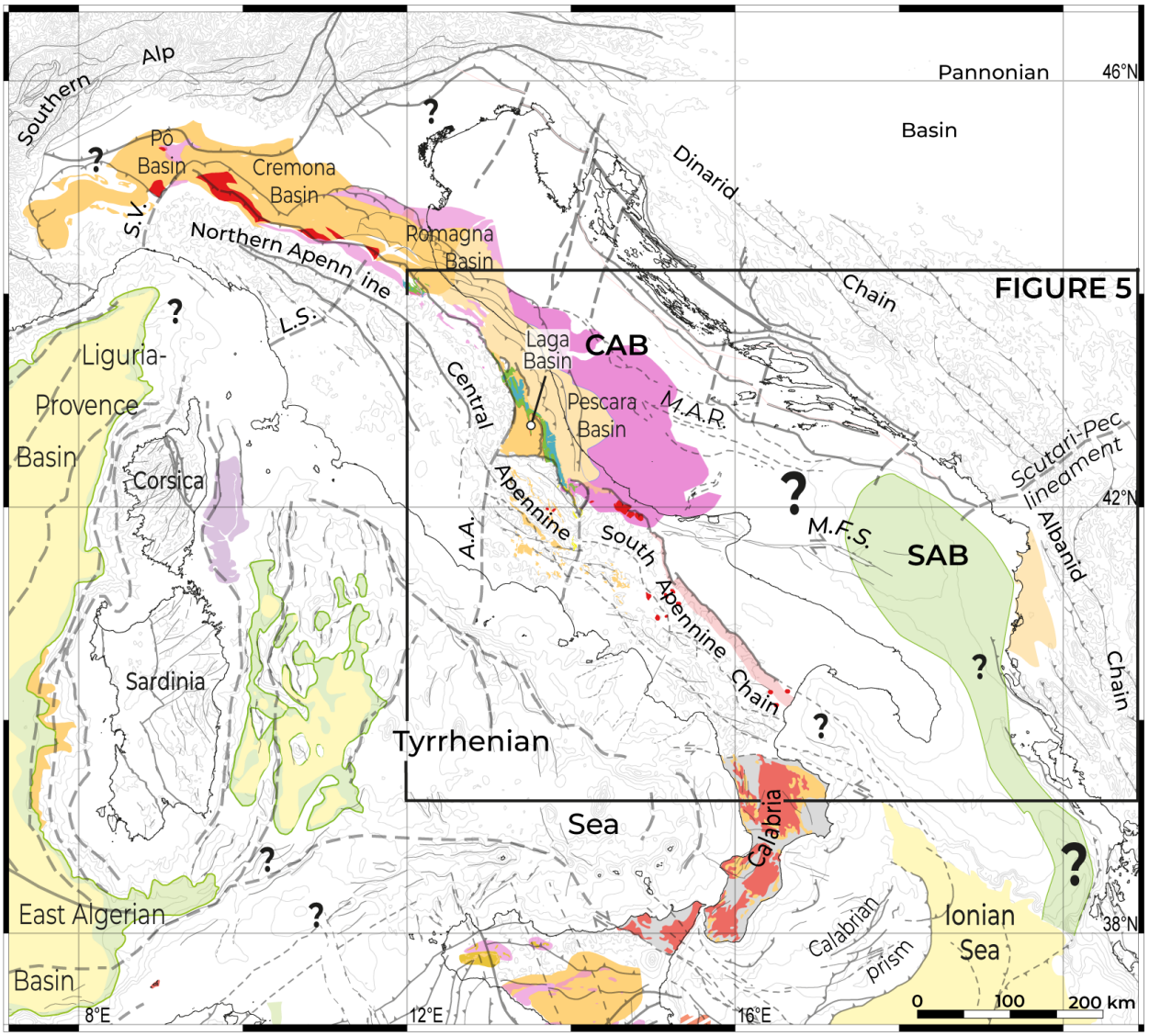

MSC formations and physiographic features

- Reworked Primary Evaporite (RLG) (Thrust top basin / On top of the autochtonous Apulian foreland).
- Primary Evaporite Fm.
- Detrital Fm. (including RLG along Apennine foredeep) (Observed / Supposed)
- 1 2 Post-evaporitic Fm. (Laga basin)
- Detrital fm. with chaotic facies (Mass Transport Deposit - MTD)
- Upper Unit
- Bedded Unit
- Mobile Unit (MSC Fm. for the East Medit. domain)

Tectonic feature

- Normal
- Transform
- Thrust
- Other fault
- Passive margin hinge line (*observed / suspected*)

1387

1388

Figure 05

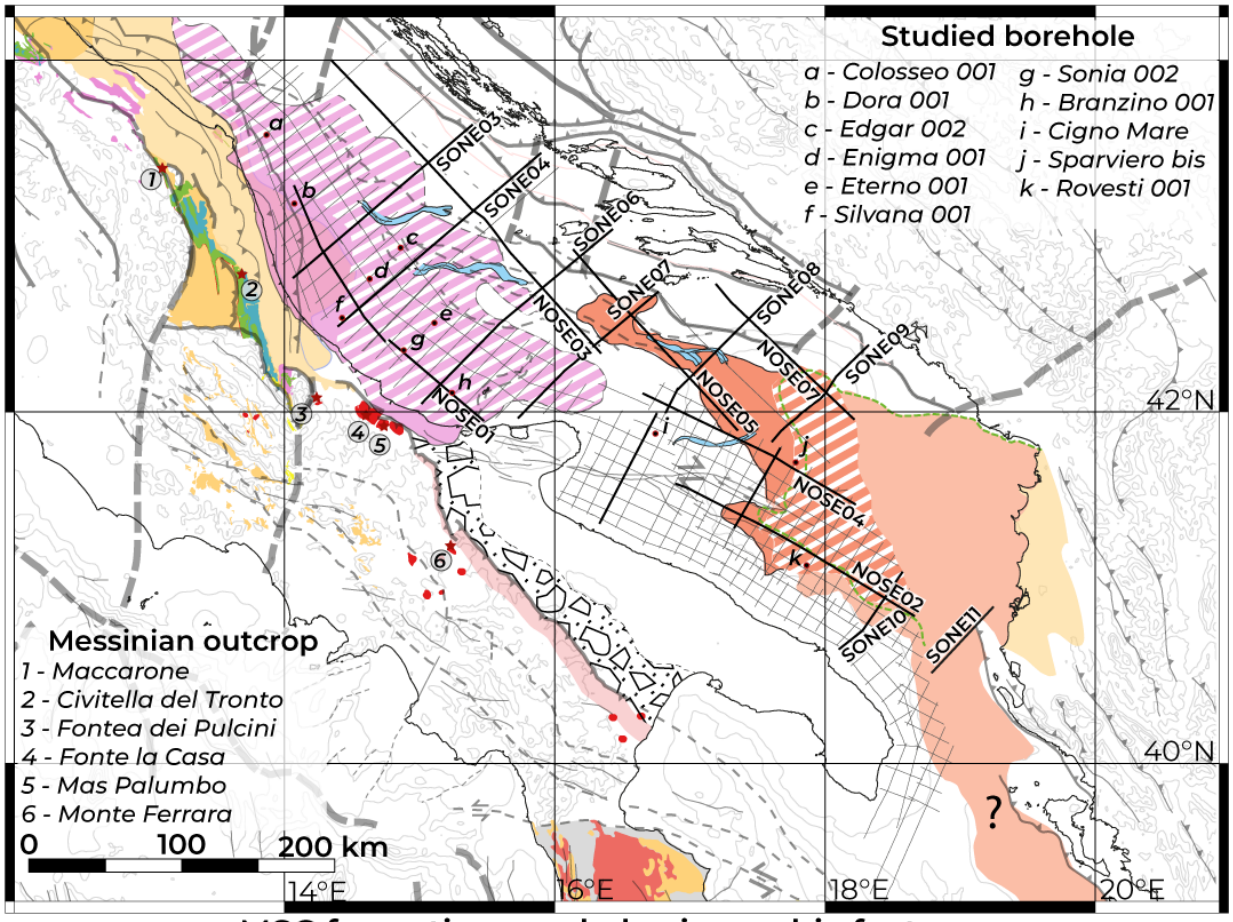

MSC formations and physiographic features

- Reworked Primary Evaporite (RLG) *(Thrust top basin / On top of the autochtonous Apulian foreland)*
- Primary Evaporite Fm.
- Primary Evaporite formation with truncation at the top of the Messinian unit
- Central-North Appennine detritic Fm.
- Post-evaporitic detritic Fm. (Laga basin)
- Conglomeratic facies at the top of Mesozoic or Miocene units.
- Detrital formation with clinoform facies (M3)
- Detrital formation with chaotic facies (M3)
- Distal detrital formation with sub-parallel reflexions *(Observed / Supposed)*
- Mobile Unit (MSC Fm. for the East Medit. domain)
- Upper limit of M4 Unit *(Proposed Upper Unit)*
- Fluvial network with direction of paleo-flows
- Seismic line
- Borehole with Gessoso Solfifera Fm.
- Messinian outcrops

Tectonic features

- Transform fault
- Thrust fault
- Normal fault
- Major fault / Hinge line

1389

1390

Figure 06A

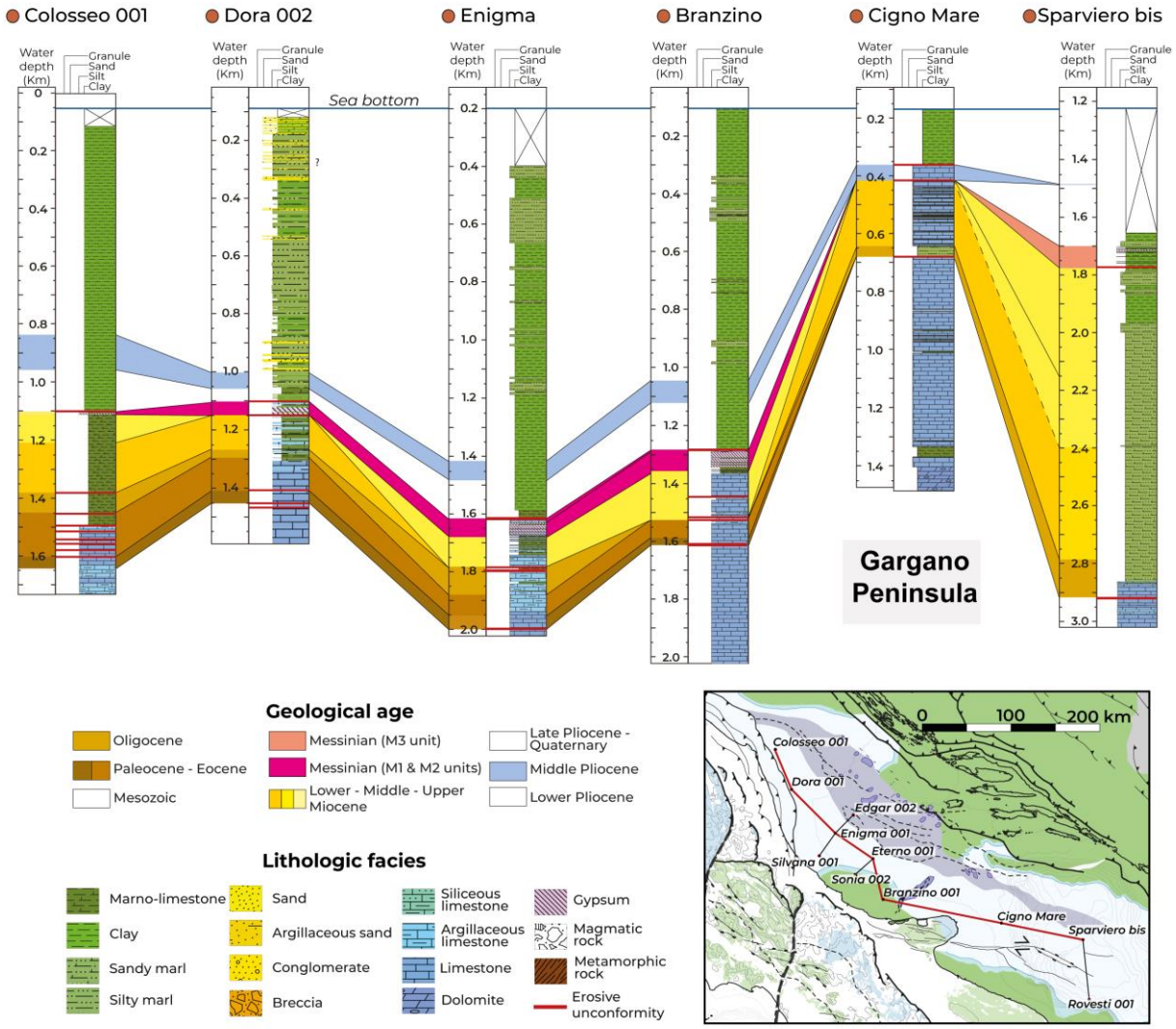

1391

Figure 06B

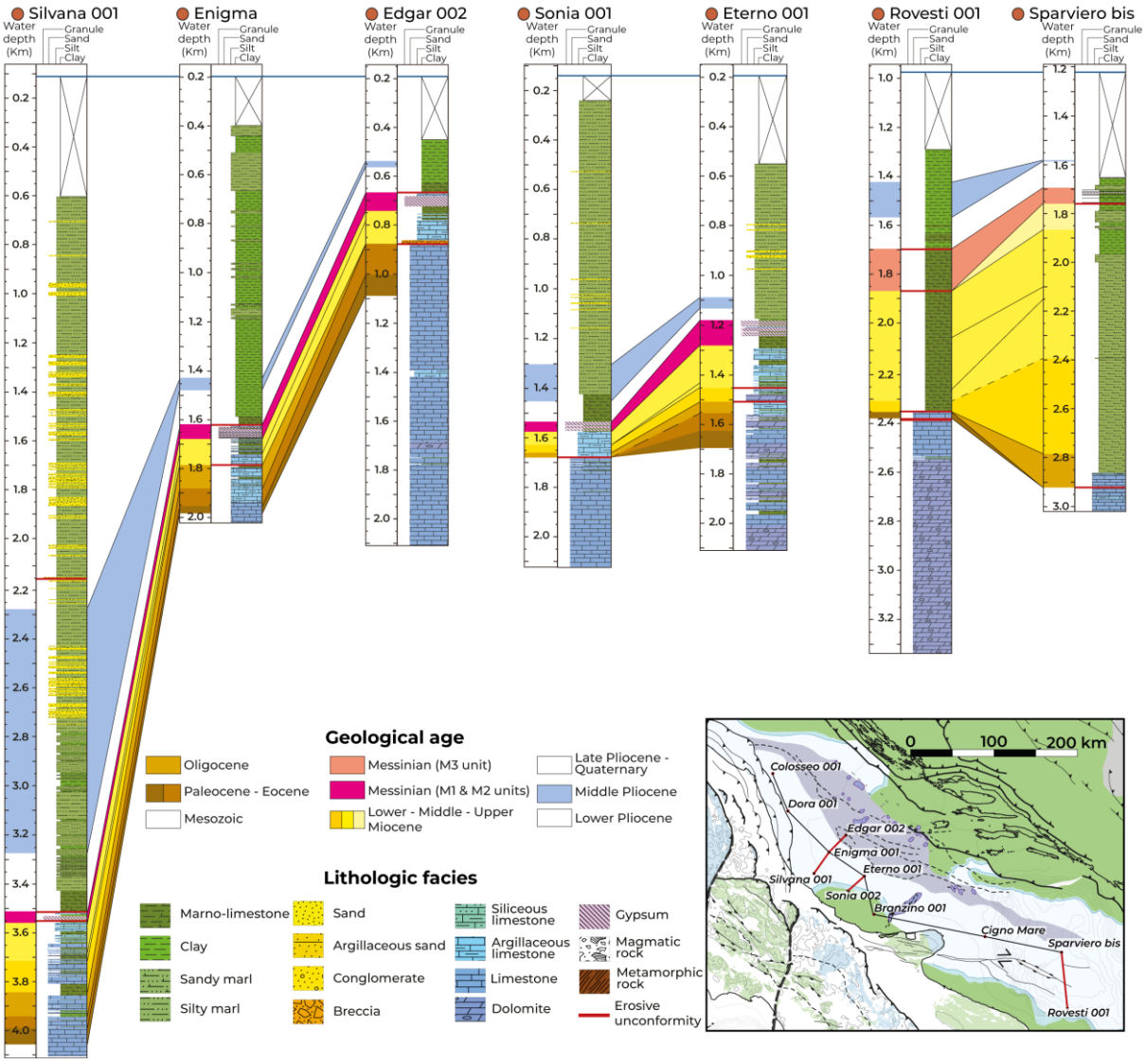
Silvana 001
Enigma
Edgar 002
Sonia 001
Eterno 001
Rovesti 001
Sparviero bis
Water depth (Km)
Granule
Sand
Silt
Clay
Geological age
Oligocene
Paleocene - Eocene
Mesozoic
Messinian (M3 unit)
Messinian (M1 & M2 units)
Lower - Middle - Upper Miocene
Late Pliocene - Quaternary
Middle Pliocene
Lower Pliocene
Lithologic facies
Marno-limestone
Clay
Sandy marl
Silty marl
Sand
Argillaceous sand
Conglomerate
Breccia
Siliceous limestone
Argillaceous limestone
Limestone
Dolomite
Gypsum
Magmatic rock
Metamorphic rock
Erosive unconformity
0
100
200 km
Colosseo 001
Dora 001
Edgar 002
Enigma 001
Eterno 001
Silvana 001
Sonia 002
Branzino 001
Cigno Mare
Sparviero bis
Rovesti 001

Figure 07

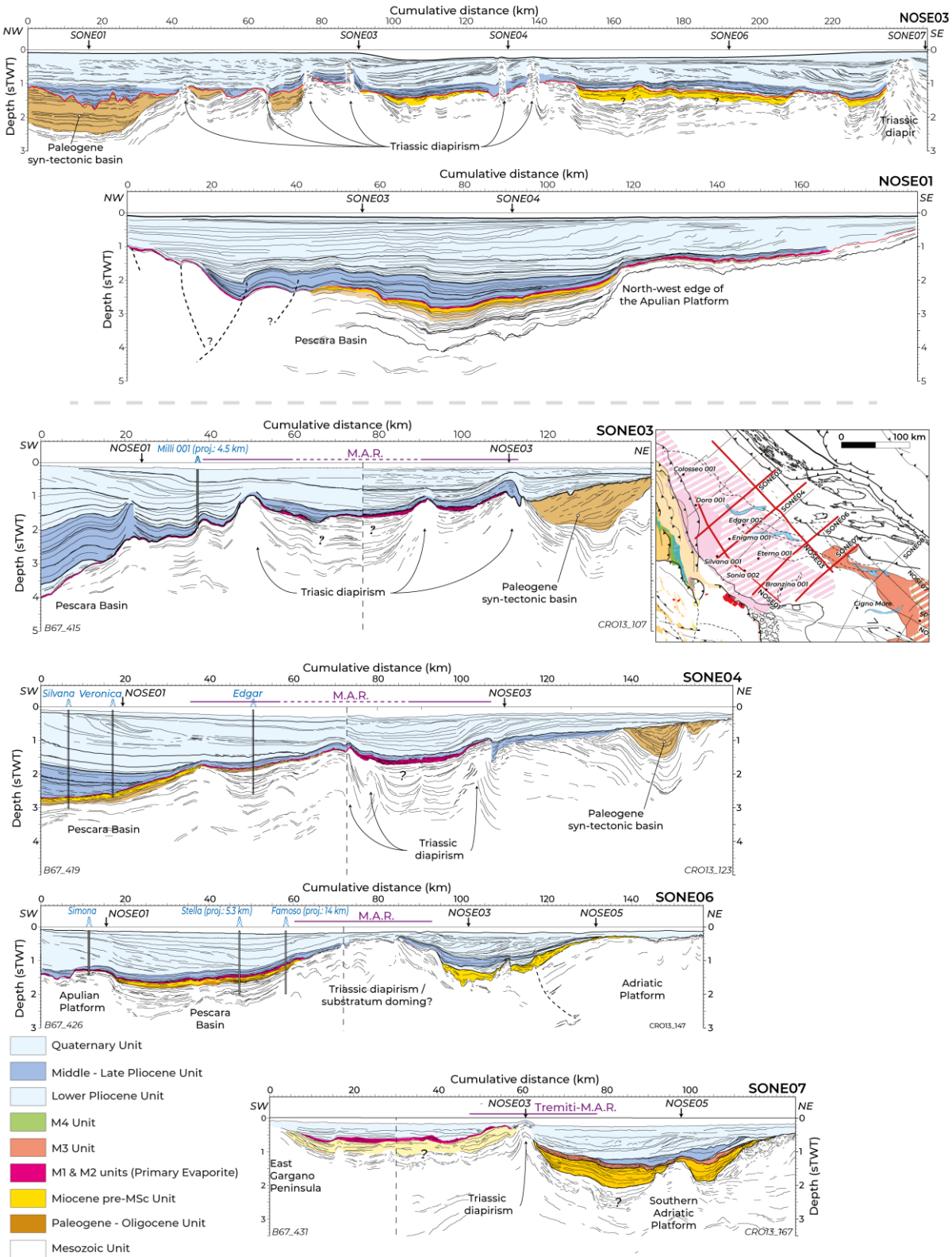
Cumulative distance (km)
NOSE03
NW
SE
SONE01
SONE03
SONE04
SONE06
SONE07
Depth (sTWT)
Paleogene
syn-tectonic basin
Triassic diapirism
Triassic
diapir
NOSE01
North-west edge of
the Apulian Platform
Pescara Basin
SONE03
SW
NE
NOSE01
Milli 001 (proj.: 4.5 km)
M.A.R.
NOSE03
Pescara Basin
Triasic diapirism
Paleogene
syn-tectonic basin
B67_415
CRO13_107
100 km
Colosseo 001
Dora 001
Edgar 002
Enigma 001
Eterno 001
Silvana 001
Sonia 002
Branzino 001
Cigno Mare
SONE04
SONE06
SONE07
NOSE03
NOSE05
SONE04
Silvana
Veronica
NOSE01
Edgar
M.A.R.
NOSE03
Pescara Basin
Triassic
diapirism
Paleogene
syn-tectonic basin
B67_419
CRO13_123
SONE06
Simona
NOSE01
Stella (proj.: 5.3 km)
Famoso (proj.: 14 km)
M.A.R.
NOSE03
NOSE05
Apulian
Platform
Pescara
Basin
Triassic diapirism /
substratum doming?
Adriatic
Platform
B67_426
CRO13_147
Quaternary Unit
Middle - Late Pliocene Unit
Lower Pliocene Unit
M4 Unit
M3 Unit
M1 & M2 units (Primary Evaporite)
Miocene pre-MSc Unit
Paleogene - Oligocene Unit
Mesozoic Unit
SONE07
NOSE03
Tremiti-M.A.R.
NOSE05
East
Gargano
Peninsula
Triassic
diapirism
Southern
Adriatic
Platform
B67_431
CRO13_167

Figure 08

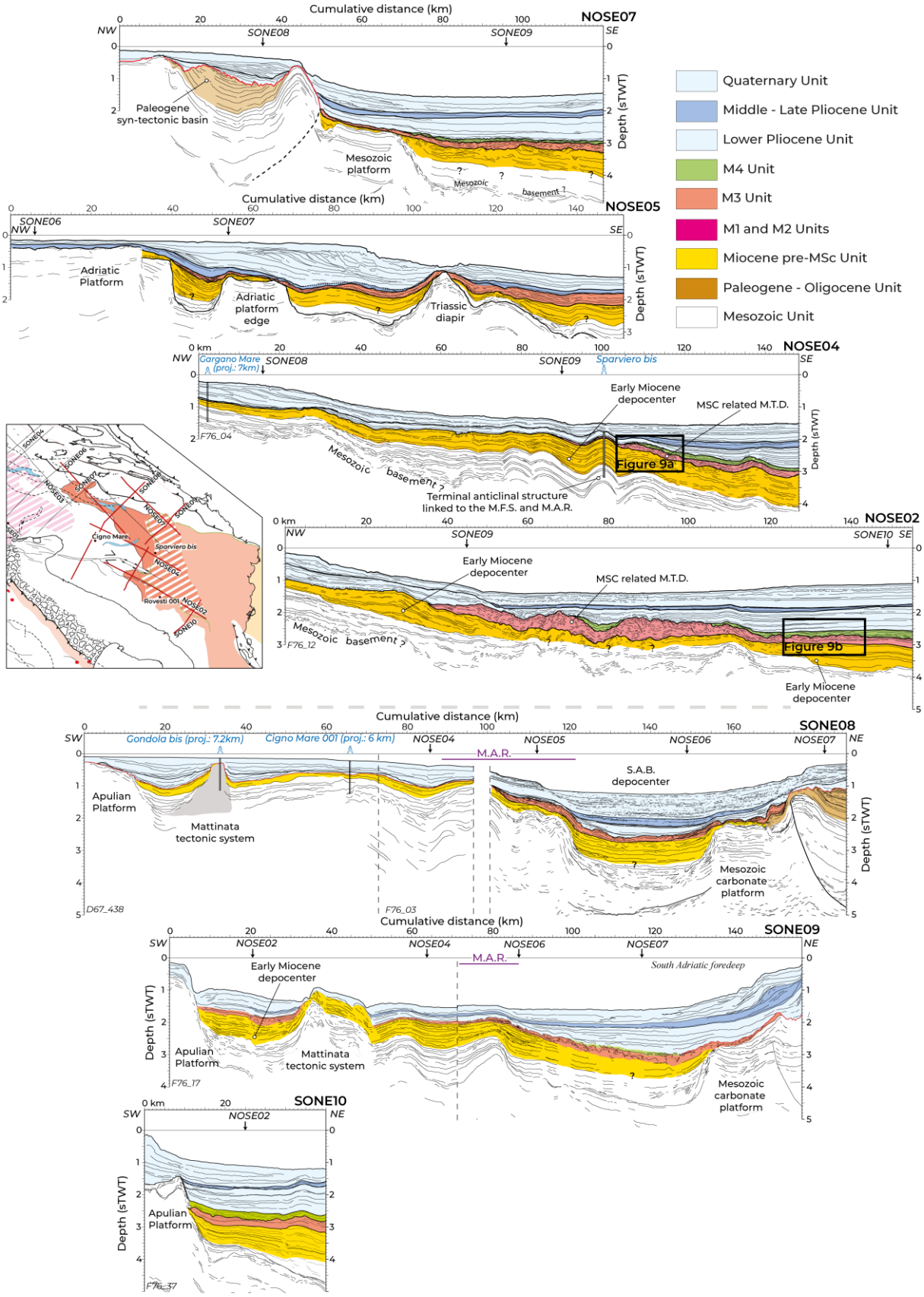
Cumulative distance (km)
NOSE07
NW
SE
SONE08
SONE09
Paleogene syn-tectonic basin
Mesozoic platform
Mesozoic basement ?
Depth (sTWT)
NOSE05
SONE06
SONE07
Adriatic Platform
Adriatic platform edge
Triassic diapir
NOSE04
Gargano Mare (proj.: 7km)
Sparviero bis
Early Miocene depocenter
MSC related M.T.D.
F76_04
Figure 9a
Terminal anticlinal structure linked to the M.F.S. and M.A.R.
NOSE02
SONE10
F76_12
Figure 9b
Cigno Mare
Rovesti 001
Gondola bis (proj.: 7.2km)
Cigno Mare 001 (proj.: 6 km)
M.A.R.
S.A.B. depocenter
Apulian Platform
Mattinata tectonic system
D67_438
F76_03
Mesozoic carbonate platform
SONE09
South Adriatic foredeep
F76_17
SONE10
F76_37
Quaternary Unit
Middle - Late Pliocene Unit
Lower Pliocene Unit
M4 Unit
M3 Unit
M1 and M2 Units
Miocene pre-MSc Unit
Paleogene - Oligocene Unit
Mesozoic Unit

Figure 09

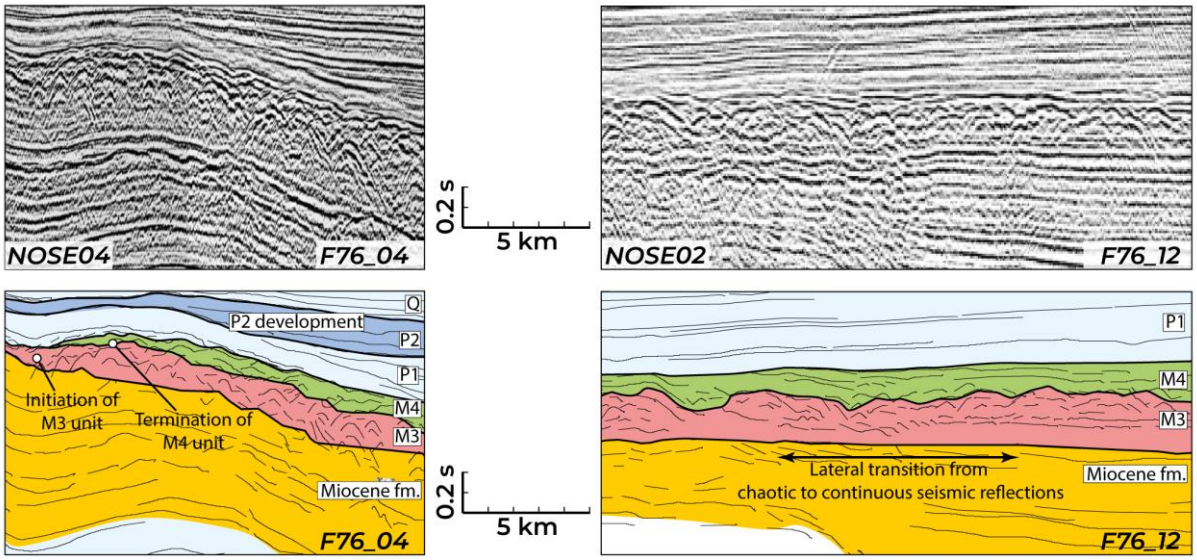
NOSE04
F76_04
0.2 s
5 km
NOSE02
F76_12
Q
P2 development
P2
P1
M4
M3
Initiation of
M3 unit
Termination of
M4 unit
Miocene fm.
F76_04
0.2 s
5 km
P1
M4
M3
Lateral transition from
chaotic to continuous seismic reflections
Miocene fm.
F76_12

Figure 10

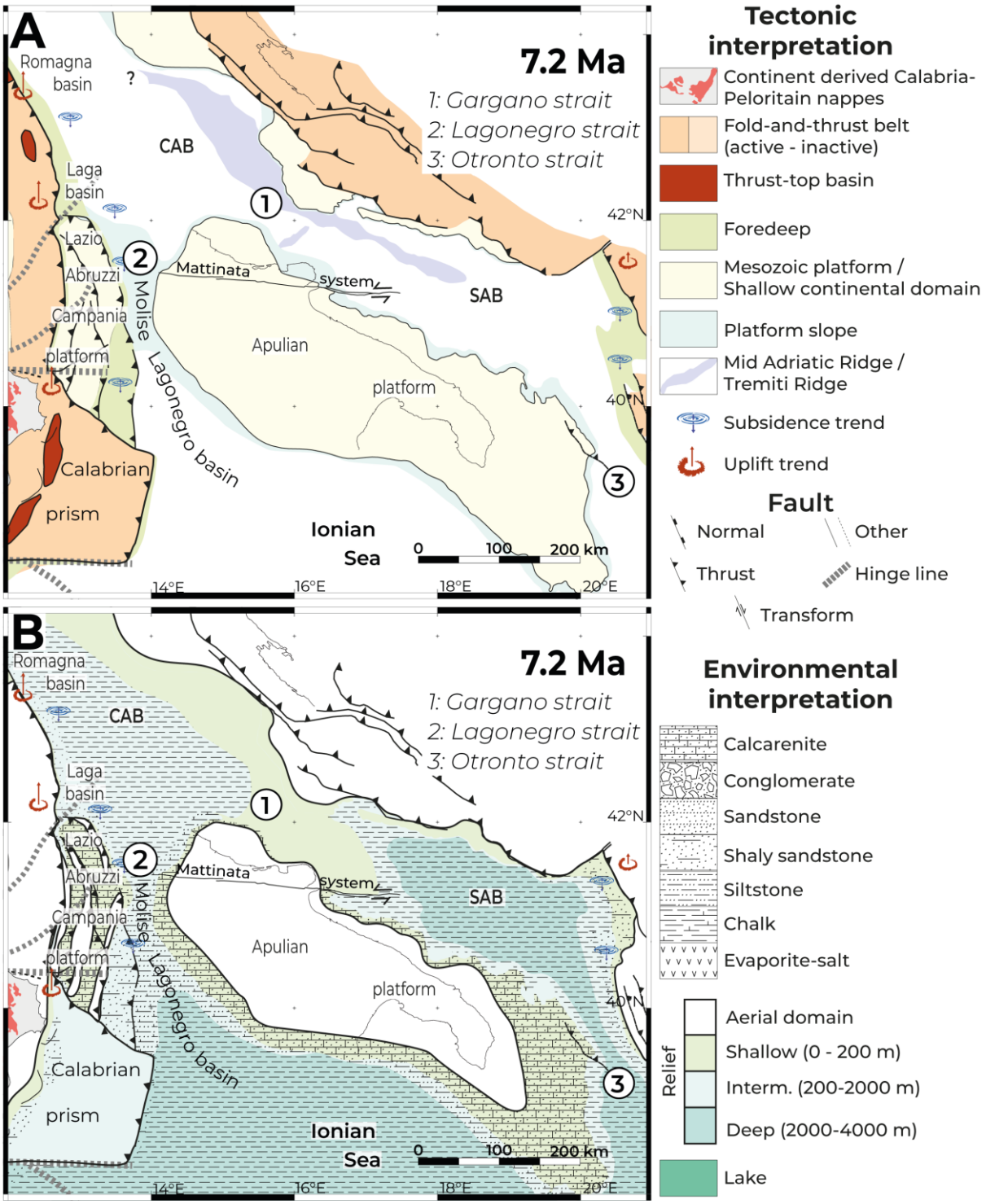
A
7.2 Ma
1: Gargano strait
2: Lagonegro strait
3: Otronto strait
Romagna basin
?
CAB
Laga basin
Lazio
Abruzzi
Campania
platform
Molise
Lagonegro basin
Mattinata
system
SAB
Apulian
platform
Calabrian
prism
Ionian
Sea
0
100
200 km
14°E
16°E
18°E
20°E
42°N
40°N
B
7.2 Ma
1: Gargano strait
2: Lagonegro strait
3: Otronto strait
Tectonic interpretation
Continent derived Calabria-Peloritain nappes
Fold-and-thrust belt (active - inactive)
Thrust-top basin
Foredeep
Mesozoic platform / Shallow continental domain
Platform slope
Mid Adriatic Ridge / Tremiti Ridge
Subsidence trend
Uplift trend
Fault
Normal
Other
Thrust
Hinge line
Transform
Environmental interpretation
Calcarenite
Conglomerate
Sandstone
Shaly sandstone
Siltstone
Chalk
Evaporite-salt
Relief
Aerial domain
Shallow (0 - 200 m)
Interm. (200-2000 m)
Deep (2000-4000 m)
Lake

1402

Figure 11

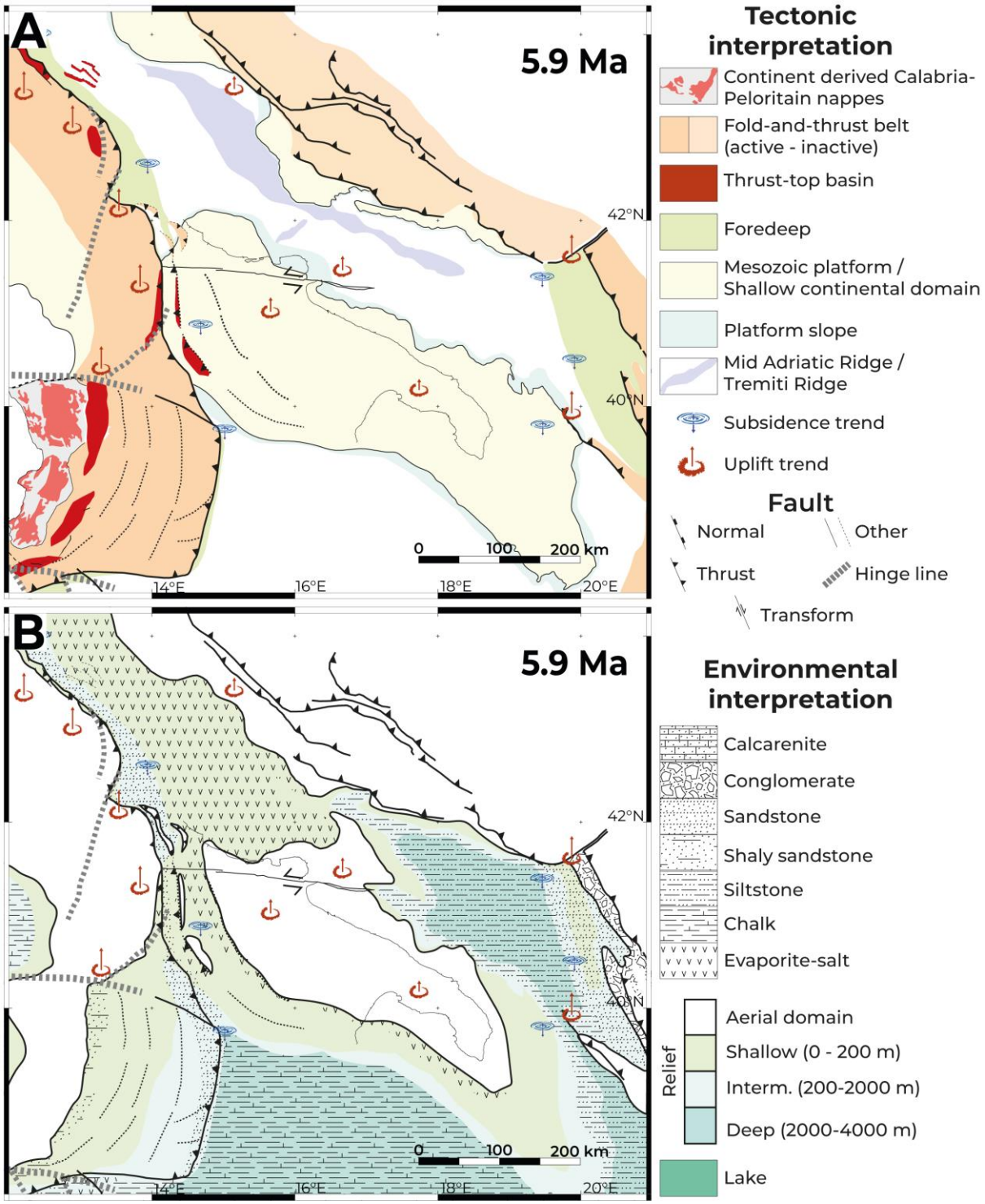

1403

1404

Figure 12

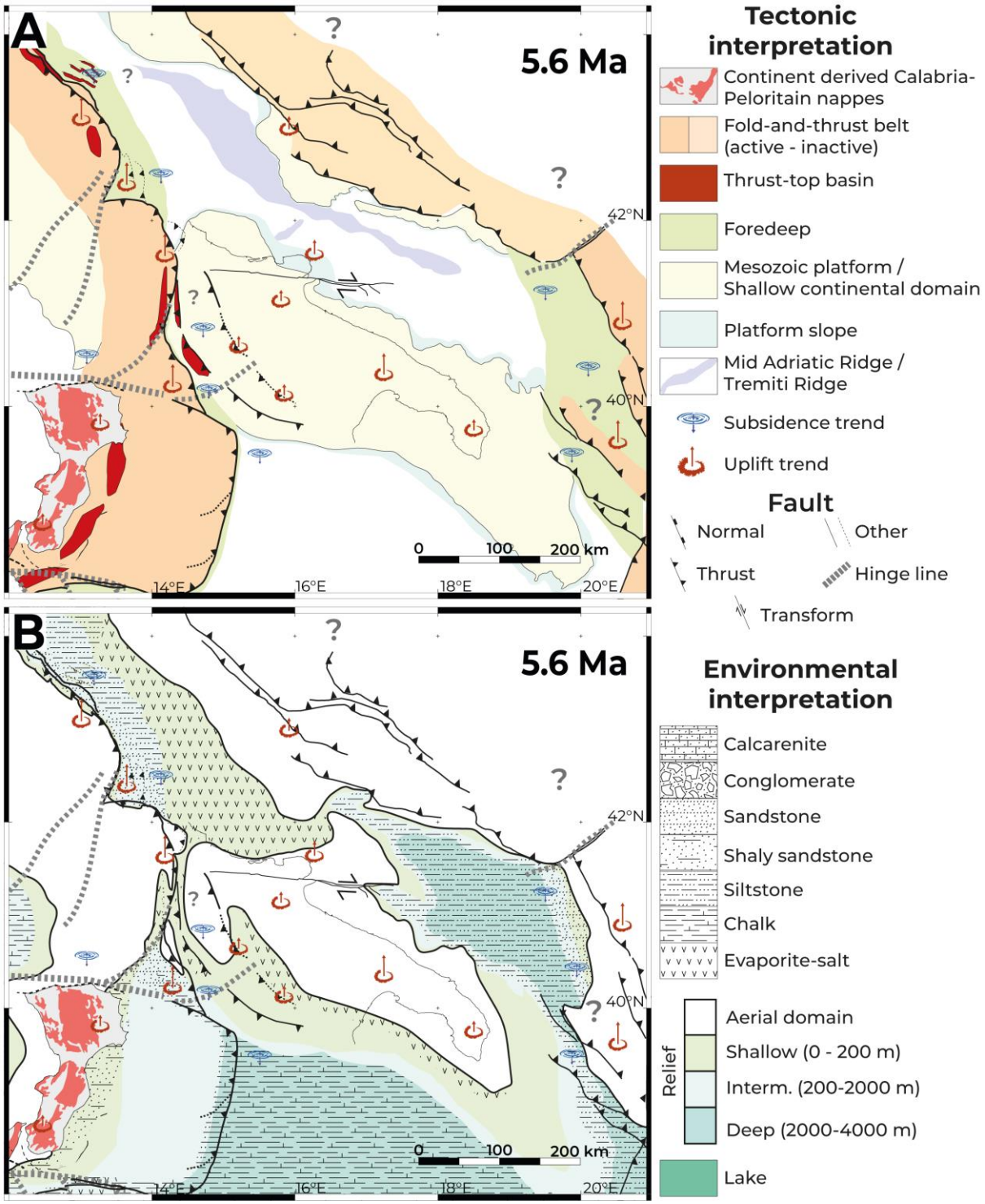

1405

1406

Figure 13

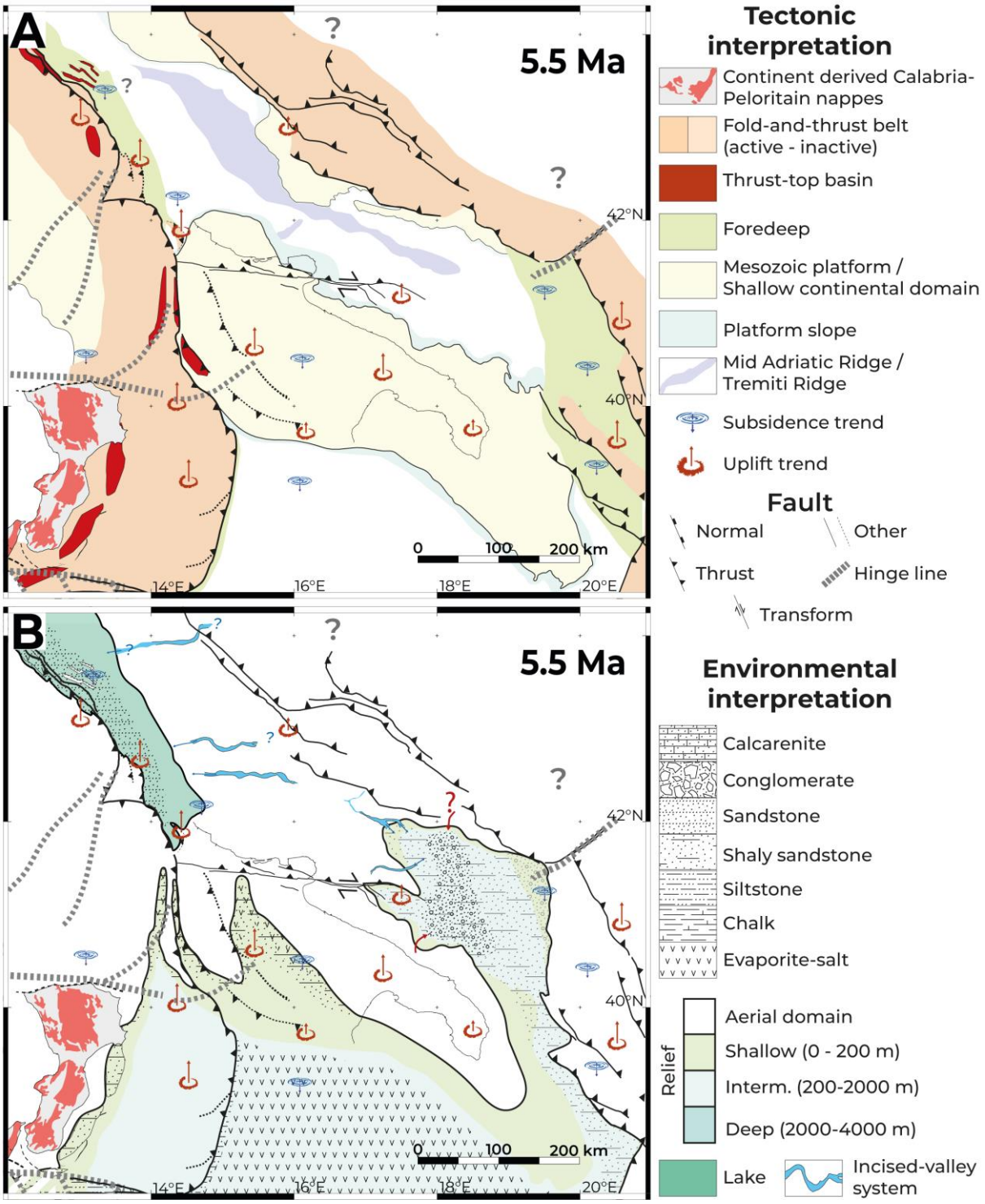

1407

1408

Figure 14

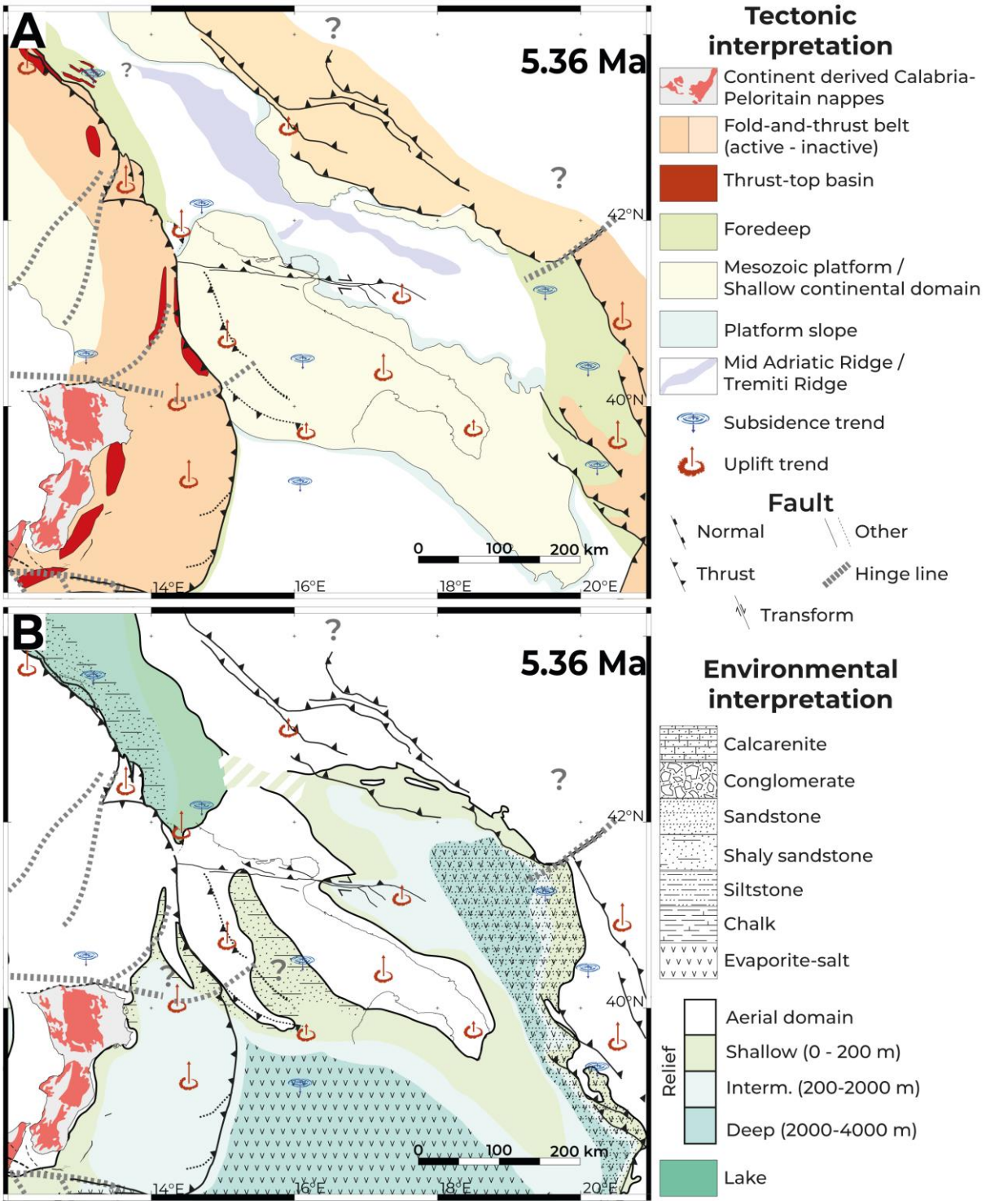

1409

1410

Figure 15

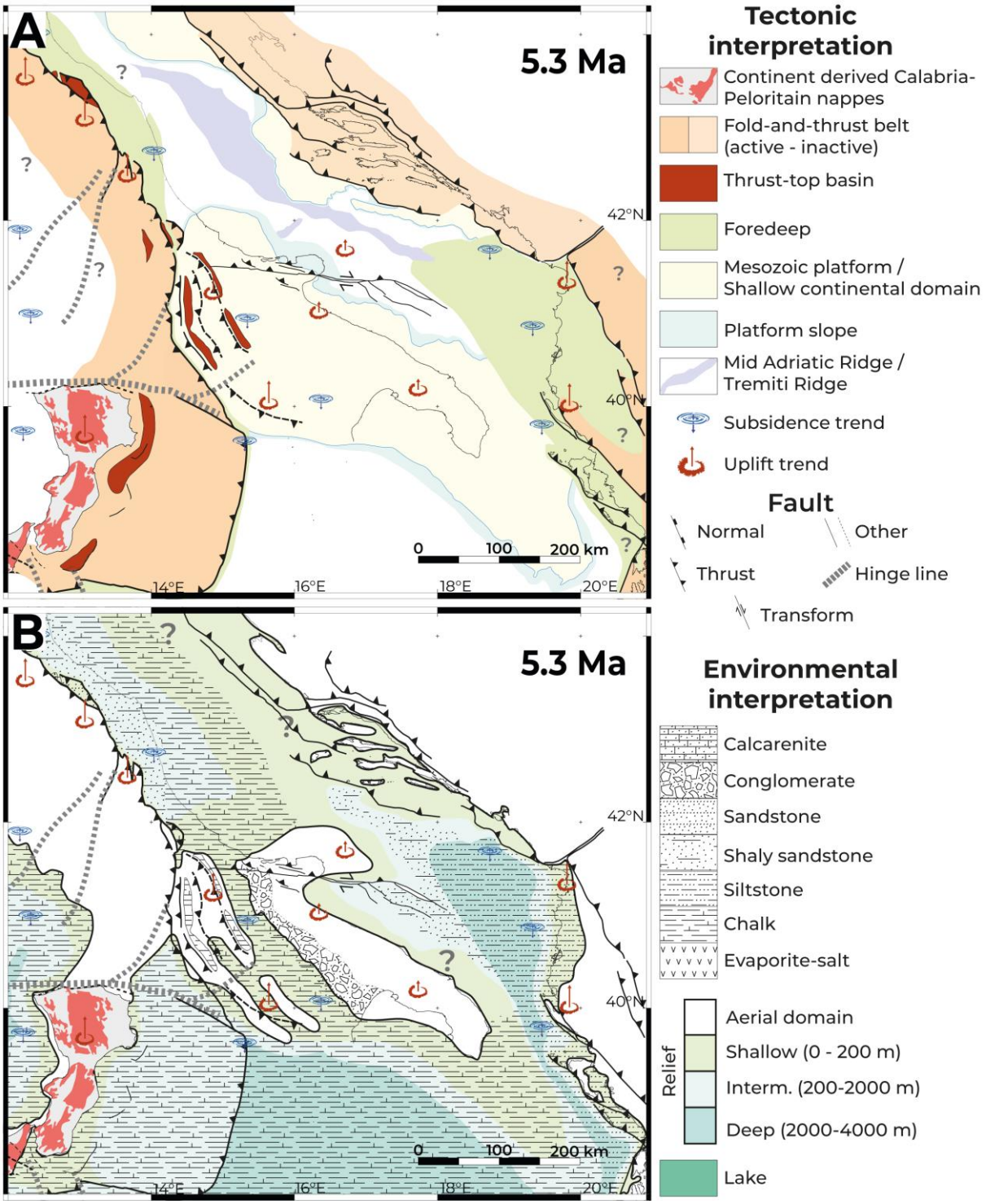

1411

1412

Figure 16

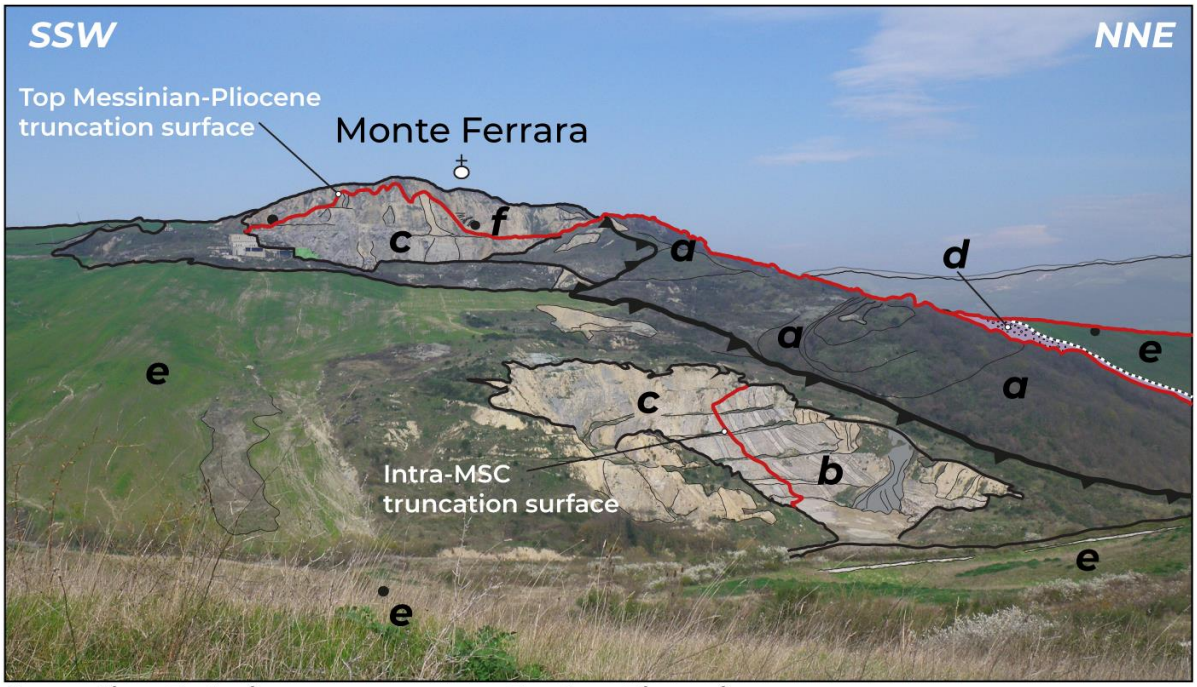

Serravallian - Tortonian

a Serra Palazzo fm. (*Serravallian - Tortonian*)

Messinian syn-MSC

b Ribboned gypsum beds (Primary Lower Gypsum)

c Reworked evapprite gypsum with PLG microblocks.

Zanclean-Piacenzian

d Conglomerate to calc-arenite formation

e Blue clay formation

Lower Pleistocene

f Stratified silt-argilleous formation

Erosive unconformity

Thrust

Biostratigraphic sample

1413

Table 01

Central Apennine stratigraphy

Pô plain		Romagna Basin			Laga Basin							
Chielmi *et al.*, 2010		Roveri et al., 2004, 2005			Artoni, 1993	Artoni, 2003	Milli et al., 2007		Centamore and Nisio, 2003			
		Marginal basins	Deep basins	Sequence	allounits	allounits	allounits	sequence	sequence		Lithostratigraphic units	
PL_1		Argile Azurre	Argile Azurre	U.B.S.U.	Unit 0	Pliocene			P1a	P1		
M_4		Colombacci fm.	Colombacci fm.	p-ev2	Colombacci unit	p-ev2	Laga 3	Cellino depositional sequence	M3b	M3	Post-evaporitic member	
M_3	LM	hiatus	S. Donato fm.	p-ev1	post-ev pelitic unit	p-ev1			M3a			
		intra-messinian unconformity	*ash layer* Sapigno fm.	MP	post-ev arenaceous fm.	post-ev arenaceous fm.			M2b	M2	Evaporitic member	
M_2		Vena del Gesso fm. (ex. Gessoso Solfifera fm. shallow water member) Autochtonous evaporite	Resedimented evaporite		Evaporitic member	ev	Laga 2		M2a			
M_1 T_2				T_2	Pre-evaporitic member	pre-ev	Laga 1	Laga depositional sequence	M1	M1	Pre-evaporitic member	
		Marnoso-arenacea fm. *'euxinic shales'*	*'euxinix shales'*		Cerrogna marls	Cerrogna marls	Cerrogna marls	Marnoso depo. seq.			Cerrogna marls and Pteropoda	
					7.25 Ma	5.97 Ma	5.6 Ma	5.42 Ma	5.33 Ma			
							U3	U4	I3			
							U2		I2			
							U1		I1			

1416

Table 02

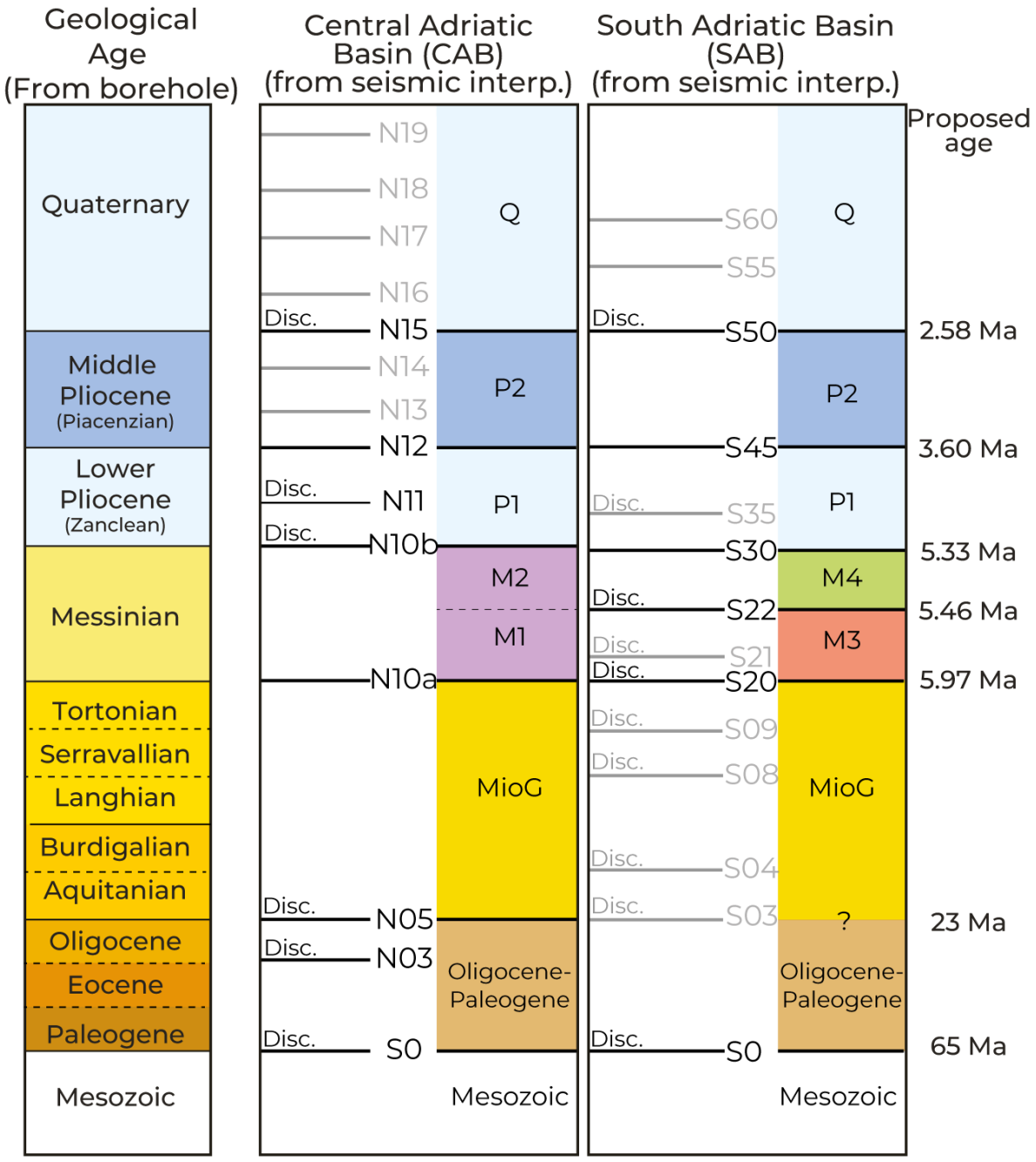

1417

Table 03

Magnetic anomaly / Aged step	Geological age (Ma)	Rotation parameters		
		Latitude	Longitude	Angle
Motion of Adria vs Eurasian plate (Sioni, 1996)				
Ano0	0.0	0	0	0
Ano6	20.0	42.8	5.1	-5.7
Motion of Calabria vs Eurasian plate (this study)				
Ano0	0.0	0	0	0
Age2.5	2.5	-14.9	-168.9	-3.0
Age4	4.0	-14.3	-170.5	-4.8
Age7.2	7.2	-14.3	-170.5	-8.7
Ano6	20.0	47.0	12.9	-47.8
Motion of Africa-Sicily vs Eurasian plate (Fidalgo, 2001)				
Ano0	0.0	0	0	0
Ano5	8.92	15.2	-20.4	-0.9
Ano6	20.0	15.0	-18.6	-2.1